Inorganic Chemistry
ARTICLE
pubs.acs.org/IC

# Synthesis and Characterization of Di- and Trivalent Pyrazolylborate $\beta$-Diketonates and Cyanometalates

Minao Tang,[‡] Dongfeng Li,[§] Uma Prasad Mallik,[†] Yuan-Zhu Zhang,[†] Rodolphe Clérac,[∥,⊥] Gordon T. Yee,[#] Myung-Hwan Whangbo,[▽] Amshumali Mungalimane,[†] and Stephen M. Holmes[*,†,‡]

[†]Department of Chemistry & Biochemistry, University of Missouri—St. Louis, St. Louis, Missouri 63121, United States
[‡]Department of Chemistry, University of Kentucky, Lexington, Kentucky 40506-0055, United States
[§]Key Laboratory of Pesticide and Chemical Biology of Ministry of Education, College of Chemistry, Central China Normal University, 430079 Wuhan, China
[∥]CNRS, UPR 8641, Centre de Recherche Paul Pascal (CRPP), Equipe "Matériaux Moléculaires Magnétiques", 115 avenue du Dr. Albert Schweitzer, F-33600 Pessac, France
[⊥]Université de Bordeaux, UPR 8641, Pessac, F-33600, France
[#]Department of Chemistry, Virginia Polytechnic and State University, Blacksburg, Virginia 24061, United States
[▽]Department of Chemistry, North Carolina State University, Raleigh, North Carolina 27695-8204, United States

Supporting Information

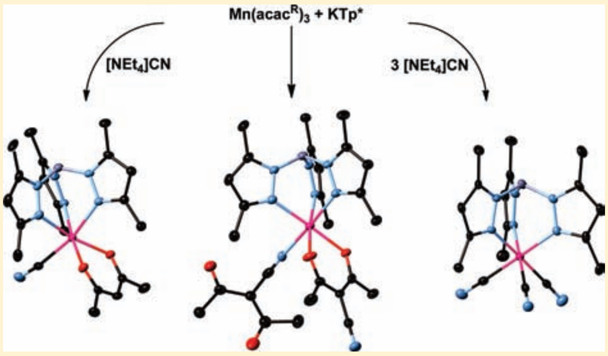

**ABSTRACT:** The syntheses, structures, and magnetic properties of a series of di- and trivalent hydridotris(3,5-dimethylpyrazol-1-yl)borate (Tp*) cyanomanganates are described. Treatment of tris(acetylacetonate)manganese(III) [Mn(acac)$_3$] with KTp* and tetra(ethyl)ammonium cyanide affords [NEt$_4$][(Tp*)Mn$^{II}$($\kappa^2$-acac)(CN)] (**1**), as the first monocyanomanganate(II) complex; attempted oxidation of **1** with iodine affords $\{$(Tp*)Mn$^{II}$($\kappa^2$-acac$^{3\text{-CN}}$)$\}_n$ (**2**) as a one-dimensional chain and bimetallic $\{$[NEt$_4$][(Tp*)Mn$^{II}$($\kappa^2$-acac$^{3\text{-CN}}$)]$_2$($\mu$-CN) (**3**) as the major and minor products, respectively. A fourth complex, [NEt$_4$][(Tp*)Mn$^{II}$($\eta^2$-acac$^{3\text{-CN}}$)($\eta^1$-NC-acac)] (**4**), is obtained via treatment of Mn(acac$^{3\text{-CN}}$)$_3$ with KTp* and [NEt$_4$]CN, while [NEt$_4$]$_2$[Mn$^{II}$(CN)$_4$] (**5**) was prepared from manganese(II) trifluoromethanesulfonate and excess [NEt$_4$]CN. Tricyanomanganate(III) complexes, [cat][(Tp*)Mn$^{III}$(CN)$_3$] [cat = NEt$_4^+$, **7**; PPN$^+$, **8**], are prepared via sequential treatment of Mn(acac$^{3\text{-CN}}$)$_3$ with KTp*, followed by [NEt$_4$]CN, or [cat]$_3$[Mn$^{III}$(CN)$_6$] with (Tp*)SnBu$_2$Cl. Magnetic measurements indicate that **1**, **2**, and **4** contain isotropic Mn$^{II}$ ($S = {}^5/_2$; $g = 2.00$) centers, and no long-range magnetic ordering is found above 1.8 K. Compounds **7** and **8** contain $S = 1$ Mn$^{III}$ centers that adopt singly degenerate spin ground states without orbital contributions to their magnetic moments.

## INTRODUCTION

Recent studies indicate that polynuclear cyanometalate complexes that contain paramagnetic centers with first-order spin−orbit coupling[1−17] exhibit fundamentally different behavior than oxide-bridged complexes,[18−29] in which the spin−orbit effect is nearly quenched by the low-symmetry ligand environment. In polynuclear cyanometalate complexes containing [M$^n$(CN)$_6$]$^{m-}$ and [(L)M$^n$(CN)$_3$]$^{m-}$ (M$^n$ = Re$^{II}$, Mo$^{III}$, Fe$^{III}$, Mn$^{III}$, etc.) ions, where L is a facially coordinated tridentate ligand, significant orbital contributions to their spin ground states are exhibited that are a necessary factor for establishing uniaxial type anisotropy and an activation energy barrier ($\Delta$) to thermal magnetization reversal, i.e. Single-Molecule Magnet (SMM) behavior.[1−17,30−36] The tripodal ligands limit the numbers and spatial arrangement of cyanide linkages formed, and via judicious choice of cyanometalate building blocks, a variety of polynuclear complexes and, in some cases, magnetic chains that exhibit slow relaxation of the magnetization may be systematically engineered.[1−17] Among these derivatives, several are reported to exhibit spin crossover,[34] superparamagnetism[1−17] and optically responsive behavior.[35] While tuning the single-ion anisotropy can in principle be accomplished via alterations of metal ions, spin state and/or orbital anisotropy in various building blocks, predicting how these single-ion properties impact overall magnetic anisotropy of the polynuclear complexes, still remains a persistent challenge.[1−17,30−40] However, the orbital contributions are often sensitive to local crystal fields, and this feature offers the

**Received:** March 7, 2011
**Published:** April 26, 2011

prospect of tuning magnetic properties at the single-ion level via distortion of the metal ion coordination spheres.[3b,10,31b]

High-spin $Mn^{III}$ ($S = 2$) ions are the most common paramagnetic ions used in the construction of oxo-carboxylate SMMs and are the principal source of their single-ion anisotropy. However, in cyanometalate chemistry, only materials containing low-spin $[Mn^{II}(CN)_6]^{4-}$ ($S = 1/2$) and $[Mn^{III}(CN)_6]^{3-}$ ($S = 1$) anions have been reported prior to our work. These cyanometalate anions exhibit first-order orbital contributions to their degenerate spin ground states and are known to efficiently engage in $\pi$ back bonding and cyanide-mediated superexchange interactions within $Mn(\mu\text{-}CN)M'$ units;[3,37−41] of these, only $[Mn^{III}(CN)_6]^{3-}$ has been used to construct discrete polynuclear complexes.

Despite reports of several cyanomanganates, most are unsuitable for constructing magnetic complexes, as they are diamagnetic. For example, dinuclear $K_4[Mn(CN)_2(NO)_2]_2$ can be prepared via treatment of $Mn(NO)_3CO$ with KCN in liquid ammonia, while a mononuclear dinitrosyl complex, $K_3[Mn(CN)_2(NO)_2]$, is obtained via reduction of the former with potassium.[42−45] A pentacyanonitrosyl complex, $K_3[Mn(CN)_5NO]$,[46−49] in addition to several carbonyl analogues of $Mn(CO)_5CN$, $K[Mn(CO)_4(CN)_2]$, $K_2[Mn(CO)_3(CN)_3]$, and $K_3[Mn(CO)_2(CN)_4]$ stoichiometry are also known;[50−54] $Na_5[Mn(CN)_6]$ is the only well-defined homoleptic diamagnetic cyanomanganate.[55−61]

Prior to 2010, there were six known *paramagnetic* cyanomanganates: $K_4[Mn^{II}(CN)_6]\cdot 3H_2O$, $Na_4[Mn^{II}(CN)_6]\cdot 10H_2O$, $K_3[Mn^{III}(CN)_6]\cdot H_2O$, $[PPN]_3[Mn^{III}(CN)_6]$, $[PPN]_2[Mn^{IV}(CN)_4]$, and $[PPN]_2[Mn^{II}(CN)_4]$.[45,62−77] The low-spin di- and trivalent hexacyanomanganates are known to exhibit low-spin $t_{2g}^5$ ($S = {}^1/_2$, $g = 2.5$)[59,66,67] and $t_{2g}^4$ ($S = 1$, $g = 2.47$)[68−77] electron configurations, respectively, with significant orbital contributions to their magnetic moments found, while tetracyanomanganate(II) complexes are magnetically isotropic ($S = {}^5/_2$, ${}^6A_1$ ground state).[76] A single pentanuclear complex, $[Mn^{II}(tmphen)]_3[Mn^{III}(CN)_6]_2$ (tmphen =3,4,7,8-tetramethyl-1,10-phenanthroline), is reported to exhibit slow relaxation of its magnetization below 1.8 K.[3]

Over the past several years, we have strived to engineer structurally related polynuclear complexes containing paramagnetic $[(Tp^R)M^n(CN)_m]^{n-m-1}$ ions, where $Tp^R$ is a pyrazolyborate anion. We have extensively utilized these di- and tricyano pyrazolylborate complexes to prepare a variety of tri-, tetra-, and octanuclear derivatives that exhibit SMM properties.[5−12] In these polynuclear complexes, we discovered that substitution at the $[(Tp^R)M^n(CN)_m]^{n-m-1}$ sites [$M^n = VO^{2+}$, $Cr^{III}$, $Fe^{III}$, $Co^{III}$] appears to be the most efficient means to tune the magnetic and optical properties.[5−12,33,35] Among known analogues, polynuclear $\{FeCo\}_n$ ($n = 2, 4$) complexes are found to exhibit thermally- and light-induced changes in their optical and magnetic properties with exceptionally long lifetimes (up to 10 y at 120 K).[35]

Much like their tricyanoferrate analogues, low spin $Mn^{II}_{LS}$ ($S = {}^1/_2$) and $Mn^{III}_{LS}$ ($S = 1$) ions are also expected to engage in efficient $\pi$ back bonding and cyanide-mediated superexchange interactions, making them attractive building blocks for the construction of polynuclear complexes, with the former ion being isoelectronic to low spin $Fe^{III}_{LS}$.[3,5−16,35−41] We reasoned that insertion of tricyanomanganate(III) ions into the trivalent sites of rectangular $\{M^{III}_2M^{II}_2\}$ and octanuclear $\{M^{III}_4M^{II}_4\}$ complexes might allow for systematic investigations into how orbital symmetry, magnetic, and optical properties change upon $M^{III}$ ion substitution in structurally related complexes.[5−16,32,33,35,36]

Unfortunately, we have been unable to find a single pyrazolylborate complex that is suitable for the preparation of any paramagnetic cyanomangante until only recently. However, given the number of known manganese $\beta$-diketonates, we turned our attention toward these reagents and investigated their usefulness for preparing $[(Tp^*)Mn^n(CN)_3]^{n-4}$ complexes.[79−84] Substituted complexes of $Mn(acac^R)_3$ ($acac^R$ = acetylacetonate, dipivaloylmethanoate, 3-cyanoacetylacetonate, etc.) stoichiometry are attractive starting materials because they are generally air and water stable soluble in a variety of organic solvents and their redox potentials can be systematically altered via introduction of various functional groups.[79−97] We reasoned that sequential substitution of acetylacetonates with pyrazolylborate anions followed by cyanide would minimize the formation of $[(Tp^*)_2Mn^n]^{n-2}$ and $[Mn^n(CN)_m]^{n-m}$ complexes and likely afford the desired tricyanomanganates. Herein, we describe the synthesis, crystallographic and magnetic characterization of several $\beta$-diketonates and their transformation into cyanomanganates.

## EXPERIMENTAL SECTION

**Materials.** All operations were conducted under an argon atmosphere using standard Schlenk and drybox techniques. Transfers of solutions containing cyanide were carried out through stainless steel cannulas. Solvents were distilled under dinitrogen from $CaH_2$ (acetonitrile, dichloromethane), sodium-benzophenone (diethyl ether), or magnesium turnings (methanol) and sparged with argon prior to use. The preparation of KTp*,[97,98] $(Tp^*)SnBu_2Cl$,[99] $K_3[Mn(CN)_6]\cdot H_2O$,[74] $[NEt_4]CN$,[100,101] 3-cyano-2,4-pentanedione ($Hacac^{3\text{-}CN}$),[78,79] tris(dipivaloylmethanato)manganese(III),[80−83] $Mn^{III}(acac)_3$,[85] $[Mn^{III}(acac^{3\text{-}CN})_3]$,[80−84] $Mn(OTf)_2$,[101] and $\{[cis\text{-}M^{II}(bipy)_2(OH_2)_2][OTf]_2\}\cdot 3H_2O$ ($M^{II}$ = Co, Ni)[102] are described elsewhere. Iodine (Baker), cobaltacene (Aldrich), and 2,2′-bipyridine (Aldrich) were used as received.

**Physical Measurements.** The IR spectra were recorded as Nujol mulls between KBr plates on Mattson Galaxy 5200 and Nicolet 6700 FTIR instruments. Magnetic measurements were conducted on a Johnson-Matthey magnetic susceptibility balance and a Quantum Design MPMS XL magnetometer. Diamagnetic corrections were estimated using Pascal's constants.[37,40] Microanalyses were performed by Robertson Microlit Laboratories.

**Synthesis of $[NEt_4][(Tp^*)Mn^{II}(\kappa^2\text{-}acac)(CN)]$ (1).** Treatment of $Mn(acac)_3$ (3.68 g, 10.5 mmol) in $CH_2Cl_2$ (20 mL) with solid KTp* (3.68 g, 11.2 mmol) rapidly afforded a brown mixture that was allowed to stir overnight. The mixture was filtered, and the brown filtrate was evacuated to dryness at room temperature. The addition of MeCN (20 mL), followed by $[NEt_4]CN$ (3.94 g, 22.4 mmol) in MeCN (20 mL), afforded a brown solution that was allowed to stir for 2 h. The solution was filtered and concentrated under vacuum conditions (*ca.* 15 mL) at room temperature. The addition of $Et_2O$ (100 mL) with stirring precipitated a pale brown residue, and subsequent rapid filtration afforded yellow crystals within 10 min upon standing. The crystals were isolated via filtration, washed with $Et_2O$ (3 × 10 mL), and dried under vacuum conditions at room temperature for 2 h. Yield: 3.52 g (55.2%). Anal. Calcd for $C_{29}H_{47}BMnN_8O_2$: C, 57.3; H, 7.80; N, 18.40. Found: C, 57.4; H, 7.88; N, 18.62. IR (Nujol, $cm^{-1}$): 3113 (s), 3067 (s), 2735 (m), 2508 (s), 2099 (m), 2076 (w), 1604 (s), 1539 (s), 1508 (s), 1450 (s), 1396 (s), 1378 (s), 1350 (s), 1248 (s), 1192 (s), 1172 (s), 1142 (m), 1065 (s), 1037 (s), 1005 (s), 980 (m), 914 (m), 859 (w), 842 (m), 804 (s), 774 (s), 750 (m), 697 (m), 653 (m), 647 (m), 534 (m), 459 (m).

**Synthesis of $\{(Tp^*)Mn^{II}(\kappa^2\text{-acac}^{3\text{-CN}})\}_n$ (2).** Treatment of **1** (1.00 g, 1.65 mmol) in MeCN (5 mL) with $I_2$ (0.211 g, 0.820 mmol) rapidly afforded a brown solution that was allowed to stand for 12 h. The yellow crystals that deposited were isolated via filtration, washed with $Et_2O$ (2 × 3 mL), and dried under vacuum conditions for 2 h at room temperature. Yield: 0.172 g (20.1%). Anal. Calcd for $C_{23}H_{31}BMnN_8O_2$: C, 53.40; H, 6.04; N, 21.66. Found: C, 53.12; H, 6.08; N, 21.44. IR (Nujol, $cm^{-1}$): 3468 (s), 3376 (s), 3251 (s), 3124 (s), 2733 (m), 2516 (s), 2452 (m), 2247 (m), 2202 (s), 2146 (m), 1634 (s), 1541 (s), 1522 (s), 1456 (s), 1417 (s), 1377 (s), 1348 (s), 1273 (m), 1196 (s), 1181 (s), 1148 (m), 1126 (m), 1067 (s), 1044 (s), 983 (m), 912 (m), 843 (m), 805 (s), 776 (m), 723 (w), 694 (m), 648 (s), 608 (w), 523 (w), 460 (m). The final yellow filtrate (from **2**) was layered with $Et_2O$ (50 mL), and the mixture was allowed to stand at room temperature for an additional 24 h. A small quantity of yellow crystals, $\{[NEt_4][(Tp^*)Mn^{II}(\kappa^2\text{-acac}^{3\text{-CN}})]_2(\mu\text{-CN})\}\cdot MeCN\cdot{}^1/_2Et_2O$ (**3**), were also isolated via filtration, washed with $Et_2O$ (2 × 5 mL), and dried under vacuum conditions for 2 h at room temperature. IR (for **3**; Nujol, $cm^{-1}$): 3363 (s), 3243 (s), 3113 (s), 2731 (m), 2517 (s), 2448 (m), 2189 (s), 2124 (m), 1624 (s), 1537 (s), 1510 (s), 1446 (s), 1378 (s), 1261 (s), 1196 (s), 1181 (s), 1068 (s), 1033 (s), 912 (m), 847 (m), 801 (s), 698 (m), 644 (s), 605 (m), 522 (m).

**Synthesis of $[NEt_4][(Tp^*)Mn^{II}(\kappa^2\text{-acac}^{3\text{-CN}})(\eta^1\text{-3-NC-acac})]\cdot MeCN\cdot{}^1/_2Et_2O$ (4).** Treatment of $Mn^{III}(acac^{3\text{-CN}})_3$ (0.331 g, 0.767 mmol) in MeOH (20 mL) with KTp* (0.253 g, 0.758 mmol) afforded a red-brown mixture that was allowed to stir overnight. The addition of $[NEt_4]CN$ (0.360 g, 2.31 mmol) in MeOH (20 mL) followed by stirring for 1 h afforded a yellow suspension that was evacuated to dryness at room temperature. The yellow residue was extracted with MeCN (15 mL) , filtered and $Et_2O$ (100 mL) was added to the brown filtrate. The deposited yellow crystals were isolated via filtration, washed with $Et_2O$ (3 × 5 mL), and dried under vacuum conditions for 2 h at room temperature. Yield: 0.150 g (25.3%). Anal. Calcd for $C_{37}H_{59}BMnN_9O_{4.5}$: C, 57.89; H, 7.75; N, 16.42. Found: C, 57.89; H, 7.56; N, 16.67. IR (Nujol, $cm^{-1}$): 3118 (m), 2737 (m), 2528 (m), 2449 (w), 2418 (w), 2256 (w), 2188 (vs), 2140 (m), 1619 (vs), 1585 (vs), 1540 (vs), 1506 (s), 1486 (vs), 1446 (vs), 1416 (vs), 1378 (vs), 1328 (vs), 1291 (s), 1199 (vs), 1124 (s), 1069 (s), 1043 (vs), 997 (s), 958 (m), 925 (s), 913 (m), 843 (m), 808 (s), 780 (s), 697 (m), 651 (s), 611 (m).

**Synthesis of $[NEt_4]_2[Mn^{II}(CN)_4]$ (5).**[103] The addition of a MeCN (10 mL) solution of $Mn(OTf)_2$ (0.200 g, 0.566 mmol) to $[NEt_4]CN$ (0.400 g, 2.56 mmol) in MeCN (10 mL) rapidly afforded a pale yellow mixture that was allowed to stir for 30 min. The mixture was concentrated under vacuum conditions at room temperature to a *ca.* 10 mL volume, and $Et_2O$ (50 mL) was layered onto the yellow solution. After 16 h, pink crystals deposited and were isolated via filtration, washed with $Et_2O$ (2 × 5 mL), and dried under vacuum conditions at room temperature for 5 min. Yield: 0.176 g (56.3%). Anal. Calcd for $C_{20}H_{40}BMnN_6$: C, 57.26; H, 9.61; N, 20.03. Found: C, 56.92; H, 9.89; N, 20.02. IR (Nujol, $cm^{-1}$): 2957 (vs), 2923 (vs), 2855 (vs), 2578 (s), 2455 (s), 2357 (s), 2311 (s), 2120 (s), 2078 (s), 1804 (m), 1678 (m), 1581 (m), 1451 (vs), 1401 (vs), 1376 (vs), 1264 (s), 1175 (vs), 1059 (s), 1010 (vs), 908 (m), 799 (vs), 723 (m), 604 (w). $\mu_{\text{eff}}(298\ K) = 5.90\ \mu_B\ (S = {}^5/_2)$

**Synthesis of $[NEt_4]_3[Mn^{III}(CN)_6]\cdot H_2O$ (6).**[103] Treatment of $K_3[Mn^{III}(CN)_6]\cdot H_2O$ (1.00 g, 2.89 mmol) with $[NEt_4]Cl\cdot H_2O$ (3.20 g, 17.4 mmol) in MeCN (25 mL) for 14 h afforded a yellow suspension that was filtered. Subsequent $Et_2O$ (100 mL) addition afforded yellow crystals after 24 h. The crystals were isolated via filtration, washed with $Et_2O$ (3 × 5 mL), and dried under vacuum conditions for 2 h at room temperature. Yield: 0.781 g (42.8%). Anal. Calcd for $C_{30}H_{62}N_9MnO$: C, 58.13; H, 10.08; N, 20.34. Found: C, 58.32; H, 10.04; N, 20.04. IR (Nujol, $cm^{-1}$): 2096 (s), 1487 (s), 1463 (s), 1440 (sh,s), 1398 (s), 1376 (m), 1364 (m), 1304 (w), 1185 (m), 1175 (s), 1056 (w), 1029 (w), 1006 (m), 793 (m), 722 (w), 467 (w).

**Synthesis of $[NEt_4][(Tp^*)Mn^{III}(CN)_3]$ (7).**[103] **Method A.** Treatment of tris(3-cyano-2,4-pentanedionato)manganese(III) (0.332 g, 0.767 mmol) in MeOH (20 mL) with KTp* (0.250 g, 0.758 mmol) afforded a brown mixture that was allowed to stir for 20 min. The addition of $[NEt_4]CN$ (0.479 g, 3.07 mmol) in MeOH (15 mL) rapidly afforded a yellow mixture that was allowed to stir an additional 1 h, was subsequently filtered, and was concentrated to *ca.* 10 mL under vacuum conditions at room temperature. The addition of $Et_2O$ (200 mL) with stirring precipitated a yellow solid that was isolated via filtration. The yellow solid was dissolved into MeCN (10 mL), and $Et_2O$ addition (20 mL) afforded yellow crystals after 24 h. The crystals were isolated via filtration, washed with $Et_2O$ (3 × 10 mL), and dried under vacuum conditions for 2 h at room temperature. Yield: 0.213 g (49.6%). Anal. Calcd for $C_{26}H_{42}BMnN_{10}$: C, 55.72; H, 7.55; N, 24.99. Found: C, 55.49; H, 7.37; N, 24.86. IR (Nujol, $cm^{-1}$): 3440 (3), 3208 (s), 2923 (vs), 2854 (vs), 2552 (s), 2113 (m), 1539 (s), 1484 (s), 1448 (s), 1415 (s), 1392 (s), 1369 (s), 1262 (m), 1200 (s), 1172 (s), 1062 (s), 1049 (s), 998 (m), 879 (w), 861 (m), 813 (m), 789 (s), 780 (s), 721 (w), 695 (m), 648 (s).

**Synthesis of $[NEt_4][(Tp^*)Mn^{III}(CN)_3]$ (7). Method B.** Treatment of $[NEt_4]_3[Mn^{III}(CN)_6]$ (0.301 g, 0.931 mmol) in $CH_2Cl_2$ (5 mL) with a $CH_2Cl_2$ (5 mL) solution of $(Tp^*)SnBu_2Cl$ (0.525 g, 0.932 mmol) afforded a yellow solution that was allowed to magnetically stir for 2 h at room temperature. The yellow mixture was concentrated to ca. 10 mL under vacuum conditions at room temperature, layered with $Et_2O$ (30 mL), and allowed to stand 1 week at −20 °C. The yellow crystals were isolated via filtration, washed with $Et_2O$ (2 × 10 mL), and dried under vacuum conditions for 2 h at room temperature. Yield: 0.113 g (29.6%). Anal. Calcd for $C_{26}H_{42}BMnN_{10}$: C, 55.72; H, 7.55; N, 24.99. Found: C, 55.32; H, 7.31; N, 24.72.

**Synthesis of $[PPN][(Tp^*)Mn^{III}(CN)_3]$ (8).** Treatment of $[PPN]_3[Mn^{III}(CN)_6]$ (0.020 g, 0.11 mmol) in $CH_2Cl_2$ (5 mL) with a $CH_2Cl_2$ (5 mL) solution of $(Tp^*)SnBu_2Cl$ (0.061 g, 0.11 mmol) afforded a yellow solution that was allowed to magnetically stir for 15 min at room temperature. The yellow mixture was layered with $Et_2O$ (30 mL) and rapidly precipitated a white solid which was removed via filtration. The filtrate was allowed to stand for 7 days, and the yellow crystals were isolated via filtration, washed with $Et_2O$ (2 × 5 mL), and dried under vacuum conditions for 2 h at room temperature. Yield: 0.037 g (35.0%). Anal. Calcd for $C_{54}H_{52}N_{10}P_2BMn$: C, 66.89; H, 5.42; N, 14.45. Found: C, 66.52; H, 5.40; N, 14.40. IR (Nujol, $cm^{-1}$): 3665 (w), 3411 (w), 3056 (s), 3077 (m), 2923 (vs), 2853 (vs), 2547 (s), 2108 (m), 1538 (s), 1482 (s), 1436 (s), 1415 (s), 1376 (s), 1285 (s), 1260 (m), 1200 (s), 1172 (s), 1114 (s), 1026 (s), 997 (m), 930 (w), 863 (m), 795 (m), 761 (s), 749 (s), 721 (w), 695 (m), 648 (s). $\mu_{\text{eff}}(298\ K) = 5.90\ \mu_B\ (S = {}^5/_2)$

**Structure Determinations and Refinements.** X-ray diffraction data for **1** and **2** were collected at 90.0(2) K on a Bruker X8 Proteum rotating anode diffractometer using graphite-monochromated Cu Kα radiation, while data for **3**−**5** and **10** were obtained at 90.0(2) K and those for **8** and **9** were obtained at 293(2) K on a Nonius kappaCCD diffractometer using Mo Kα radiation. Crystals were mounted in Paratone-N oil on glass fibers. Initial cell parameters were obtained (DENZO)[104] from ten 1° frames (SCALEPACK).[104] Lorentz/polarization corrections were applied during data reduction. The structures were solved by direct methods (SHELXL97)[105] and completed by difference Fourier methods (SHELXL97).[105] Refinement was performed against $F^2$ by weighted full-matrix least-squares (SHELXL97),[105] and empirical absorption corrections (either SCALEPACK[104] or SADABS[106]) were applied. Hydrogen atoms were found in difference maps and subsequently placed at calculated positions using suitable riding models with isotropic displacement parameters derived from their carrier atoms. Non-hydrogen atoms were refined with anisotropic displacement parameters. Atomic scattering factors were taken from the *International Tables for Crystallography Vol. C.*[107] Crystal data, relevant details of the

**Table 1. Crystallographic Data for $[NEt_4][(Tp^*)Mn^{II}(\kappa^2\text{-acac})(CN)]$ (1), $\{(Tp^*)Mn^{II}(\kappa^2\text{-acac}^{3\text{-}CN})\}_n$ (2), $\{[NEt_4][(Tp^*)Mn^{II}(\kappa_2\text{-acac}^{3\text{-}CN})]_2(\mu\text{-}CN)\}\cdot MeCN\cdot {}^1/_2Et_2O$ (3), $[NEt_4][(Tp^*)Mn^{II}(\kappa^2\text{-acac}^{3\text{-}CN})(\eta^1\text{-acac}^{3\text{-}CN})]\cdot MeCN\cdot {}^1/_2Et_2O$ (4), $[NEt_4]_2[Mn^{II}(CN)_4]$ (5), $[PPN][(Tp^*)Mn^{III}(CN)_3]$ (8), $[Cp_2Co^{III}]_4[Mn^{II}(CN)_6]\cdot 2H_2O$ (9), and $[\mathit{cis}\text{-}Co^{III}(CN)_2(bpy)_2]$-$[OTf]\cdot MeCN$ (10)**

| | 1 | 2 | 3 | 4 | 5 | 8 | 9 | 10 |
|---|---|---|---|---|---|---|---|---|
| formula | $C_{29}H_{49}BMnN_8O_2$ | $C_{23}H_{31}BMnN_8O_2$ | $C_{55}H_{59}BMnN_9O_{4.5}$ | $C_{37}H_{59}BMnN_9O_{4.5}$ | $C_{20}H_{40}MnN_6$ | $C_{54}H_{52}BMnN_{10}P_2$ | $C_{46}H_{40}Co_4MnN_6O_2$ | $C_{25}H_{19}CoF_3N_7O_3S$ |
| fw | 607.51 | 517.31 | 1186.89 | 767.68 | 419.52 | 968.75 | 999.50 | 613.46 |
| cryst syst | monoclinic | monoclinic | triclinic | monoclinic | monoclinic | triclinic | tetragonal | monoclinic |
| space group | $P2_1/n$ | $P2_1/c$ | $P\bar{1}$ | $P2_1/n$ | $C2/c$ | $P\bar{1}$ | $I\bar{4}$ | $C2/c$ |
| wavelength, $\lambda$ | 1.54178 | 1.54178 | 0.71073 | 0.71073 | 0.71073 | 0.71073 | 0.71073 | 0.71073 |
| temp., K | 90.00(2) | 90.00(2) | 90.0(2) | 90.00(2) | 90.00(2) | 293(2) | 293(2) | 90.00(2) |
| $a$, Å | 11.4389(5) | 13.7449(3) | 11.3921(1) | 9.6732(2) | 15.4590(4) | 9.7995(2) | 13.026(2) | 15.282(3) |
| $b$, Å | 22.3832(1) | 7.9023(2) | 15.0378(2) | 23.2168(4) | 10.3260(3) | 15.7266(3) | 13.026(2) | 14.216(3) |
| $c$, Å | 12.9427(6) | 24.6315(6) | 19.0437(2) | 18.5506(4) | 15.6990(5) | 16.3355(4) | 13.993(3) | 12.110(2) |
| $\alpha$, deg | 90.0 | 90.0 | 87.6479(4) | 90.0 | 90.0 | 84.4993(8) | 90.00 | 90 |
| $\beta$, deg | 92.026(2) | 101.228(1) | 77.8182(4) | 98.0310(9) | 99.175(1) | 85.7660(8) | 90.00 | 109.58(3) |
| $\gamma$, deg | 90.0 | 90.0 | 83.1053(4) | 90.0 | 90.0 | 82.9083(9) | 90.00 | 90.00 |
| $V$, Å$^3$ | 3311.8(3) | 2624.2(2) | 3165.48(6) | 4125.3(1) | 2474.0(1) | 2481.84(9) | 2374.2(7) | 2478.8(9) |
| $D_c$, g cm$^{-3}$ | 1.218 | 1.309 | 1.245 | 1.236 | 1.126 | 1.296 | 1.398 | 1.644 |
| $Z$ | 4 | 4 | 2 | 4 | 4 | 2 | 8 | 4 |
| $\mu$, mm$^{-1}$ | 3.536 | 4.378 | 0.456 | 0.370 | 0.549 | 0.378 | 1.668 | 0.844 |
| $R_1$[a] | 0.0839 | 0.0358 | 0.0576 | 0.0389 | 0.0426 | 0.0567 | 0.0783 | 0.1015 |
| w$R_2$[a] | 0.2706 | 0.0876 | 0.1443 | 0.0889 | 0.0939 | 0.1520 | 0.2306 | 0.2977 |

[a] $I > 2\sigma(I)$, $R_1 = \Sigma||F_o| - |F_c||/\Sigma|F_o|$, $wR_2 = [\Sigma w(F_o^2 - F_c^2)^2/\Sigma w(F_o^2)^2]^{1/2}$.

**Table 2. Selected Bond Distances (Å) for $[NEt_4][(Tp^*)Mn^{II}(\kappa^2\text{-acac})(CN)]$ (1), $\{(Tp^*)Mn^{II}(\kappa^2\text{-acac}^{3\text{-}CN})\}_n$ (2), $\{[NEt_4][(Tp^*)Mn^{II}(\kappa_2\text{-acac}^{3\text{-}CN})]_2(\mu\text{-}CN)\}\cdot MeCN\cdot {}^1/_2Et_2O$ (3), and $[NEt_4][(Tp^*)Mn^{II}(\kappa^2\text{-acac}^{3\text{-}CN})(\eta^1\text{-acac}^{3\text{-}CN})]\cdot MeCN\cdot {}^1/_2Et_2O$ (4)**

| 1 | | 2 | | 3 | | | | 4 | |
|---|---|---|---|---|---|---|---|---|---|
| Mn1−C16 | 2.248(8) | Mn1−N7A | 2.315(2) | Mn1−N14(C43) | 2.241(4) | Mn2−N14(C43) | 2.241(4) | Mn1−N8 | 2.256(2) |
| Mn1−O1 | 2.162(5) | Mn1−O1 | 2.156(1) | Mn1−O1 | 2.164(2) | C17−C18 | 1.407(6) | Mn1−O1 | 2.159(1) |
| Mn1−O2 | 2.227(5) | Mn1−O2 | 2.195(1) | Mn1−O2 | 2.171(2) | C18−C19 | 1.426(6) | Mn1−O2 | 2.178(2) |
| Mn1−N1 | 2.286(5) | Mn1−N1 | 2.226(2) | Mn1−N1 | 2.335(3) | O1−C19 | 1.261(5) | Mn1−N1 | 2.220(2) |
| Mn1−N3 | 2.281(5) | Mn1−N3 | 2.196(2) | Mn1−N3 | 2.221(3) | O2−C17 | 1.250(4) | Mn1−N3 | 2.229(2) |
| Mn1−N5 | 2.263(5) | Mn1−N5 | 2.213(2) | Mn1−N5 | 2.217(3) | C38−C39 | 1.407(7) | Mn1−N5 | 2.240(2) |
| O1−C18 | 1.259(8) | O1−C17 | 1.246(2) | Mn1−C43(N14) | 2.249(3) | C39−C40 | 1.419(7) | O1−C17 | 1.253(2) |
| O2−C20 | 1.264(8) | O2−C19 | 1.248(2) | Mn2−O3 | 2.144(3) | O3−C40 | 1.261(5) | O2−C19 | 1.253(2) |
| C18−C19 | 1.40(1) | C17−C18 | 1.433(3) | Mn2−O4 | 2.152(3) | O4−C38 | 1.257(5) | C17−C18 | 1.427(3) |
| C19−C20 | 1.40(1) | C18−C19 | 1.432(3) | Mn2−N7 | 2.357(3) | C21−N13 | 1.147(6) | C18−C19 | 1.429(3) |
| C16−N7 | 1.15(1) | C21−N7 | 1.150(3) | Mn2−N9 | 2.215(3) | C42−N15 | 1.144(6) | C21−N7 | 1.148(3) |
| | | Mn···Mn | 9.08(3) | Mn2−N11 | 2.256(3) | C43−N14 | 1.151(4) | C27−N8 | 1.092(3) |

structure determinations, and selected geometrical parameters are provided in Tables 1−4 (for **1**−**5** and **8**−**10**).

## RESULTS AND DISCUSSION

**Synthesis and Spectroscopic Characterization: Divalent Complexes.** Our initial studies investigated the conversion of tris(acetylacetonato)manganese(III) and its conversion to other pyrazolylborate complexes in polar organic solvents. Treatment of $Mn(acac)_3$ with potassium hydridotris(3,5-dimethylpyrazolyl)borate [KTp*] in dichloromethane affords a red-brown precipitate and supernatant whose infrared spectra suggest that $[(Tp^*)Mn(acac)_n]$ fragments are present. The infrared spectrum of this mixture contains strong $\bar{\nu}_{BH}$ absorptions that are shifted to higher energies [2512 and 2522 cm$^{-1}$] relative to KTp* [2436 cm$^{-1}$],[97] while additional and intense $\bar{\nu}_{CO}$ absorptions consistent with the presence of coordinated acetylacetonates are also present.[81,108] The absence of pyrazole $\bar{\nu}_{C=N}$ stretches near ca. 1575 cm$^{-1}$ suggests that the Tp* ligands are three-coordinate in the soluble and insoluble fractions.[97,98] Assuming that the energy of the $\bar{\nu}_{BH}$ tracks with the overall charge of the complex, the dichloromethane-insoluble material is probably cationic [$\bar{\nu}_{BH}$ = 2522 cm$^{-1}$], while the soluble fraction likely contains a neutral complex [$\bar{\nu}_{BH}$ = 2512 cm$^{-1}$].[97,98] Further assuming that each fraction contains $[(Tp^*)Mn^{III}(acac)_n]^{n-2}$ ions, we tentatively propose that the soluble and insoluble compounds have

**Table 3. Selected Bond Angles (deg) for [$NEt_4$][(Tp*)$Mn^{II}$($\kappa^2$-acac)(CN)] (1), {(Tp*)$Mn^{II}$($\kappa^2$-$acac^{3\text{-}CN}$)}$_n$ (2), {[$NEt_4$][(Tp*)$Mn^{II}$($\kappa_2$-$acac^{3\text{-}CN}$)]$_2$($\mu$-CN)}·MeCN·$^1/_2Et_2O$ (3), and [$NEt_4$][(Tp*)$Mn^{II}$($\kappa^2$-$acac^{3\text{-}CN}$)($\eta^1$-$acac^{3\text{-}CN}$)]·MeCN·$^1/_2Et_2O$ (4)**

| 1 | | 2 | | 3 | | 4 | |
|---|---|---|---|---|---|---|---|
| N1−Mn1−C16 | 171.5(2) | N1−Mn1−N7A | 96.38(6) | N1−Mn1−C43 | 179.2(1) | N1−Mn1−N8 | 94.21(7) |
| N1−Mn1−N3 | 80.7(2) | N1−Mn1−N3 | 85.42(6) | N1−Mn1−N3 | 82.38(9) | N1−Mn1−N3 | 86.43(6) |
| N1−Mn1−N5 | 82.2(2) | N1−Mn1−N5 | 86.60(6) | N1−Mn1−N5 | 95.7(1) | N1−Mn1−N5 | 81.74(6) |
| N1−Mn1−O1 | 94.0(2) | N1−Mn1−O1 | 175.51(5) | N1−Mn1−O1 | 90.86(9) | N1−Mn1−O1 | 95.05(6) |
| N1−Mn1−O2 | 89.1(2) | N1−Mn1−O2 | 94.70(5) | N1−Mn1−O2 | 89.46(9) | N1−Mn1−O2 | 173.66(6) |
| O1−Mn1−O2 | 83.3(2) | O1−Mn1−O2 | 80.93(5) | O1−Mn1−O2 | 81.8(1) | O1−Mn1−O2 | 81.05(5) |
| Mn1−C16−N7 | 176.5(6) | Mn1−N7−C21 | 155.0(2) | Mn1−C43−N14 | 173.1(3) | Mn1−N8−C27 | 170.8(2) |
| O1−C18−C19 | 126.2(7) | O1−C17−C18 | 124.0(2) | O1−C19−C18 | 124.2(4) | O1−C17−C18 | 123.5(2) |
| O2−C20−C19 | 127.0(6) | O2−C19−C18 | 124.1(2) | O2−C19−C18 | 127.4(4) | O2−C19−C18 | 124.1(2) |
| C18−C19−C20 | 125.8(6) | C17−C18−C19 | 124.8(2) | C17−C18−C19 | 125.7(4) | C17−C18−C19 | 125.2(2) |
| | | C18−C21−N7 | 178.2(2) | N7−Mn2−N14 | 176.3(1) | C18−C21−N7 | 179.1(3) |
| | | C19−C18−C21 | 117.8(2) | N7−Mn2−N9 | 81.2(1) | O3−C23−C24 | 124.3(2) |
| | | C17−C18−C21 | 117.3(2) | N7−Mn2−N11 | 81.9(1) | O4−C25−C24 | 121.0(2) |
| | | | | N7−Mn2−O3 | 90.3(1) | C23−C24−C25 | 127.2(2) |
| | | | | N7−Mn2−O4 | 90.3(1) | C23−C24−C27 | 117.1(2) |
| | | | | Mn2−N14−C43 | 177.5(3) | C25−C24−C27 | 115.6(2) |
| | | | | O3−Mn2−O4 | 81.7(1) | | |
| | | | | O3- C40−C39 | 123.7(4) | | |
| | | | | O4−C38−C39 | 124.4(4) | | |
| | | | | C38−C39−C40 | 125.5(4) | | |

**Table 4. Selected Bond Distances (Å) and Angles (deg) for [$NEt_4$]$_2$[$Mn^{II}(CN)_4$] (5), [PPN][(Tp*)$Mn^{III}(CN)_3$] (8), [$Cp_2Co^{III}$]$_4$[$Mn^{II}(CN)_6$]·$2H_2O$ (9), and [*cis*-$Co^{III}(CN)_2(bpy)_2$][OTf]·MeCN (10)**

| 5 | | 8 | | 9 | | 10 | |
|---|---|---|---|---|---|---|---|
| Mn1−C1 | 2.137(2) | Mn1−C1 | 1.982(3) | Mn1−C1 | 1.982(8) | Co1−N1 | 1.936(5) |
| Mn1−C2 | 2.151(2) | Mn1−C2 | 1.986(3) | Mn1−C2 | 1.989(8) | Co1−N2 | 1.964(5) |
| C1−N1 | 1.152(3) | Mn1−C3 | 1.980(3) | Mn1−C1A | 1.982(8) | Co1−N1A | 1.936(5) |
| C2−N2 | 1.144(3) | Mn1−N5 | 2.022(2) | Mn1−C1B | 1.960(7) | Co1−N2A | 1.963(5) |
| | | Mn1−N7 | 2.049(2) | Mn1−C1C | 1.960(7) | Co1−C11 | 1.876(6) |
| | | Mn1−N9 | 2.032(2) | Mn1−C2A | 1.98(1) | Co1−C11A | 1.876(6) |
| | | C1−N1 | 1.160(4) | C1−N1 | 1.175(9) | C11−N3 | 1.155(8) |
| | | | | C2−N2 | 1.14(2) | | |
| C1−Mn1−C2 | 111.47(7) | C1−Mn1−C2 | 87.8(1) | C1−Mn1−C2 | 179.6(6) | N1−Co1−N2 | 82.8(2) |
| Mn1−C1−N1 | 178.3(2) | C1−Mn1−C3 | 86.2(1) | Mn1−C1−N1 | 179.1(9) | N1A−Co1-N2A | 82.8(2) |
| Mn1−C2−N2 | 177.7(2) | C2−Mn1−C3 | 88.5(1) | Mn1−C2−N2 | 180.000(1) | C11−Co1−C11A | 89.0(4) |
| C1−Mn1−C1A | 111.5(1) | C1−Mn1−N5 | 93.7(1) | C1−Mn1−C1C | 90.001(2) | Co1−C11−N3 | 179.4(6) |
| C1−Mn1−C2A | 108.06(8) | C1−Mn1−N7 | 177.4(1) | | | | |
| | | C1−Mn1−N9 | 92.2(1) | | | | |
| | | N5−Mn1−N7 | 88.8(1) | | | | |
| | | N5−Mn1−N9 | 88.1(1) | | | | |
| | | N7−Mn1−N9 | 88.6(1) | | | | |

[(Tp*)$Mn^{III}(acac)_2$] and [(Tp*)$Mn^{III}$(acac)](acac) formulations, respectively.

Unfortunately, attempts to isolate and structurally characterize these intermediate complexes consistently met with failure, and we elected to use the pyrazolylborate/$Mn(acac)_3$ mixtures *in situ* in subsequent reactions. Sequential treatment of $Mn(acac)_3$ with KTp*, followed by excess tetra(ethyl)ammonium cyanide [$NEt_4CN$], affords [$NEt_4$][(Tp*)$Mn^{II}$($\kappa^2$-acac)(CN)] (**1**) as a yellow crystalline solid. Attempted oxidation of **1** with molecular iodine yields {[(Tp*)-$Mn^{II}$($\kappa^2$-$acac^{3\text{-}CN}$)]}$_n$ (**2**) and {[$NEt_4$][(Tp*)$Mn^{II}$($\kappa^2$-$acac^{3\text{-}CN}$)]$_2$-($\mu$-CN)}·MeCN·$^1/_2Et_2O$ (**3**) as the major and minor products, respectively, while air exposure of **1**−**3** affords intractable mixtures. We presume that electrophillic iodination of **1** followed by rapid cyanide substitution affords **2** and **3**, rather than the desired neutral trivalent [(Tp*)$Mn^{III}$($\kappa^2$-acac)(CN)] complex.

The infrared spectra of **1** and **2** exhibit intense cyanide stretching absorptions that are shifted to higher energies relative to tetra(ethyl)ammonium cyanide (2056 $cm^{-1}$)[100,101] and most cyanomanganates. For **1**, the $\bar{\nu}_{CN}$ absorptions [2099 and 2076 $cm^{-1}$)] are in the range seen for $K_4[Mn^{II}(CN)_6]\cdot 3H_2O$

(2060 cm$^{-1}$), $[Mn^{II}(CN)_2(bipy)_2]\cdot 3H_2O$ [2114 cm$^{-1}$], and $[NEt_4]_2[Mn^{II}(CN)_4]$ (**5**, below) [2120 and 2078 cm$^{-1}$], suggesting that Mn$^{II}$ ions and efficient $\pi$ back bonding interactions are present.[41,59,61−77,102,108] For **2**, the $\bar{\nu}_{CN}$ stretches [2247, 2202, and 2146 cm$^{-1}$] are comparable to those seen in infrared spectra of $K_2[Mn^{IV}(CN)_6]$[75,108] (2240, 2150 cm$^{-1}$), $Mn^{III}(acac^{3\text{-}CN})_3$[80,83] [2211 cm$^{-1}$], and 3-cyano-2,4-pentanedione[78,79] (2217 cm$^{-1}$) but are far from those in **1** and a variety of cyanomanganates: $[PPN]_2[Mn^{IV}(CN)_6]$ (2132 cm$^{-1}$), $[PPN]_3[Mn^{III}(CN)_6]$ (2092 and 2098 cm$^{-1}$), $K_3[Mn^{III}(CN)_6]$ (2112 and 2121 cm$^{-1}$), and $K_2Mn^{II}[Mn^{II}(CN)_6]$ (2055 cm$^{-1}$).[41,75,77,108,109] The infrared spectrum of **2** also contains intense $\bar{\nu}_{CO}$ stretches that are shifted to higher energies relative to those seen for **1**. The highest energy $\bar{\nu}_{CN}$ absorptions in **2** [2247 and 2202 cm$^{-1}$] are likely due to coordinated $\kappa^2$:$\eta^1$-acac$^{3\text{-}CN}$ ligands spanning adjacent Mn$^{II}$ centers, while the lowest energy $\bar{\nu}_{CN}$ [2146 cm$^{-1}$] stretches belong to nitrile-like terminal 3-cyano groups.[41,108,109]

As judged from the energies and numbers of $\bar{\nu}_{CN}$ stretches present in the infrared spectrum of **3** [2189 and 2124 cm$^{-1}$], we propose that organic nitriles *and* anionic cyanides are likely present.[110] The highest energy $\bar{\nu}_{CN}$ stretching absorption is in the range expected for organic nitrile groups, while the latter stretch is comparable to those seen for $K_2Mn^{II}[Mn^{II}(CN)_6]$ (2055 cm$^{-1}$), $Mn^{II}_3[Mn^{III}(CN)_6]\cdot 12H_2O$ (2148 cm$^{-1}$), and $CsMn^{II}[Mn^{III}(CN)_6]\cdot {}^1/_2H_2O$ [2148 cm$^{-1}$ (Mn$^{III}$($\mu$-CN)Mn$^{II}$)].[41,108,109] The lowest energy $\bar{\nu}_{CN}$ [2124 cm$^{-1}$] is most consistent with the presence of Mn$^{II}$($\mu$-CN)Mn$^{II}$ linkages, and we propose that inefficient charge delocalization (via $\pi$ back bonding) in **3** affords a higher energy cyano stretching absorption relative to those reported for $K_2Mn^{II}[Mn^{II}(CN)_6]$.[41,108,109]

Realizing that the manganese centers are reduced during the above reactions (likely by cyanide), we investigated the reactivity of several substituted $Mn(acac^R)_3$ complexes with KTp*. Treatment of $Mn(acac^R)_3$ (acac$^R$ = 3-cyano-2,4-pentanedionato, acac$^{3\text{-}CN}$) with methanolic KTp*, followed by [NEt$_4$]CN, affords $[NEt_4][(Tp^*)Mn^{II}(\kappa^2\text{-}acac^{3\text{-}CN})(\eta^1\text{-}NC\text{-}acac)]\cdot MeCN\cdot {}^1/_2Et_2O$ (**4**) as the major product. Subsequent treatment of **4** in methanol with excess [NEt$_4$]CN affords $[NEt_4][(Tp^*)Mn^{III}(CN)_3]$ (**7**) in moderate yield; efforts to isolate the putative divalent tricyano intermediate have been unsuccessful to date. In an attempt to simplify the preparation of **7**, we reasoned that if pyrazolylborate stannyl reagents [e.g., (Tp*)SnBu$_2$Cl]$^{99}$ can effectively substitute coordinated halides for Tp* anions, then pseudohalide complexes (such as cyanometalates) should undergo analogous transformations. Indeed, treatment of $[cat]_3[Mn^{III}(CN)_6]$ with (Tp*)SnBu$_2$Cl in dichloromethane affords $[cat][(Tp^*)Mn^{III}(CN)_3]$ complexes (**7**, NEt$_4^+$; **8**, PPN$^+$, bis(triphenyl)phosphine iminium) in modest crystalline yields.

The infrared spectra of **4**, **7**, and **8** contain high-energy $\bar{\nu}_{BH}$ and $\bar{\nu}_{CN}$ stretching absorptions that are shifted to higher energies relative to those seen for **1**−**3**. For **4**, the $\bar{\nu}_{BH}$ [2528 cm$^{-1}$] and $\bar{\nu}_{CN}$ absorptions [2188 and 2140 cm$^{-1}$] indicate that organic nitriles and coordinated Tp* ligands are present.[108] Likewise, the infrared spectra of **7** and **8** also contain intense $\bar{\nu}_{BH}$ [2552 and 2547 cm$^{-1}$] stretches at considerably higher energies than those seen for **1**−**3**, suggesting that trivalent manganese ions are also present. Consistent with this assumption, the $\bar{\nu}_{CN}$ [2113 and 2108 cm$^{-1}$] absorptions seen for **6** and **7** are comparable to those found for $[PPN]_3[Mn^{III}(CN)_6]$ [2092 and 2098 cm$^{-1}$] and $K_3[Mn^{III}(CN)_6]$ [2112 and 2121 cm$^{-1}$] and are far from those reported for $[PPN]_2[Mn^{IV}(CN)_6]$ (2132 cm$^{-1}$) and $K_2[Mn^{IV}(CN)_6]$ (2150 cm$^{-1}$).[41,45,59,75,77,108] From the infrared data, we conclude that **7** and **8** contain trivalent manganese centers.

While investigating the cyanide substitution chemistry of manganese complexes, we also discovered an improved and direct method for the preparation of a homoleptic tetracyanomanganate(II) complex. Treatment of manganese(II) trifluoromethanesulfonate with four equivalents of [NEt$_4$]CN in acetonitrile cleanly affords $[NEt_4]_2[Mn^{II}(CN)_4]$ (**5**) as pale yellow crystals. The infrared spectrum of **5** exhibits two strong $\bar{\nu}_{CN}$ stretching absorptions [2120 and 2078 cm$^{-1}$] that are markedly different in energy than those reported for a variety of cyanomanganates: $K_4[Mn^{II}(CN)_6]\cdot 10H_2O$ [2036 cm$^{-1}$], $[PPN]_2[Mn^{II}(CN)_4]$ (2209 cm$^{-1}$), $[PPN]_2[Mn^{IV}(CN)_6]$, and $[PPN]_3[Mn^{III}(CN)_6]$.[45,59,66,75−77,108] The $\bar{\nu}_{CN}$ energies seen for **5** are comparable to that found for $[Mn^{II}(CN)_2(bpy)_2]\cdot 3H_2O$ [2114 cm$^{-1}$].[102] As judged from the energy of the $\bar{\nu}_{CN}$ in the infrared spectrum of **5**, we propose that those reported for $[PPN]_2[Mn^{II}(CN)_4]$[76] are most likely due organic nitriles (e.g., MeCN), rather than coordinated anionic cyanides.[103]

Unfortunately, attempts to prepare additional divalent cyanomanganates from **1**−**8** using a variety of reagents and reaction conditions has, to date, afforded a plethora of undesirable reaction products. For example, air exposure to **1**−**5** affords intractable mixtures, while treatment of **5** with KTp* or (Tp*)SnBu$_2$Cl consistently affords $[(Tp^*)_2Mn^{II}]$, [NEt$_4$]CN, and KCN as the major reaction products. Likewise, attempts to prepare $[(Tp^*)Mn^{II}(CN)_3]^{2-}$ via treatment of **7** or **8** with cobaltacene in acetonitrile or dichloromethane affords mixtures of $[(Tp^*)_2Mn^{II}]$[110] [$\bar{\nu}_{BH}$ = 2523 cm$^{-1}$] and $[Cp_2Co^{III}]_4[Mn^{II}(CN)_6]\cdot 2H_2O$ (**9**), with the energy of the $\bar{\nu}_{CN}$ stretching absorption [$\bar{\nu}_{CN}$ = 2098 cm$^{-1}$] appearing in the range expected for divalent hexacyanometalates;[45,59,66,90] intractable mixtures are also obtained when **7** is treated with Na/Hg amalgams.

Attempted insertion of **7** and **8** into the trivalent sites of $\{Mn^{III}_2M^{II}_2\}$ square complexes (M$^{II}$ = Mn, Co, Ni) at room temperature were met with limited success due to redox and cyanide redistribution reactions. For example, treatment of **7** with $[\textit{cis}\text{-}Co^{II}(bpy)_2(OH_2)_2][OTf]_2$ cleanly affords $[\textit{cis}\text{-}Co^{III}(CN)_2(bpy)_2][OTf]$ (**10**, $\bar{\nu}_{CN}$ = 2142 cm$^{-1}$) in dimethylformamide, rather than the desired $\{Mn^{III}_2Co^{II}_2\}$ complex. Likewise, under identical reaction conditions, a combination of **7** and $[Ni^{II}(bpy)_2(OH_2)_2][OTf]_2$ rapidly precipitates a white to colorless solid whose infrared spectrum exhibits a medium intensity $\bar{\nu}_{BH}$ stretch [2521 cm$^{-1}$]; single crystal diffraction studies of these crystals verify that $[(Tp^*)_2Mn]$ has formed.[85] Additional and intense $\bar{\nu}_{CN}$ absorptions [2139 and 2150 cm$^{-1}$] are also found in reaction mixture residues containing **7** and $[Ni^{II}(bpy)_2(OH_2)_2][OTf]_2$ and are tentatively attributed to Ni$^{II}$($\mu$-CN)M$^{II}$ linkages derived from $[Ni^{II}(CN)_4]^{2-}$ ions [$\bar{\nu}_{CN}$ = 2124 cm$^{-1}$].[111,112] Unfortunately, all attempts to obtain structural data of the putative cyanide-bridged polynuclear tetracyanonickelate have been unsuccessful.

Reasoning that ligand substitution and redistribution would proceed more slowly at lower reaction temperatures (−40 °C), we reinvestigated the reaction chemistry of **7** with anhydrous divalent triflates and 2,2′-bipyridine mixtures. Indeed treatment of **7** with manganese(II) and nickel(II) trifluoromethanesulfonates in the presence of 2,2′-bipyridine affords tetranuclear complexes of $\{[(Tp^*)Mn^{III}(CN)_3]_2[M^{II}(bpy)_2]_2[OTf]_2\}\cdot$2DMF stoichiometry (M$^{II}$ = Mn, Ni).[103] Surprisingly, analogous efforts to prepare $\{Mn^{III}_2Co^{II}_2\}$ complexes consistently met with failure. For example, treatment of **7** with $[\textit{cis}\text{-}Co^{II}(bpy)_2(OH_2)_2][OTf]_2$ at or below room temperature cleanly affords $[\textit{cis}\text{-}Co^{III}(CN)_2(bpy)_2][OTf]\cdot MeCN$ (**10**; $\bar{\nu}_{CN}$ = 2142 cm$^{-1}$) as

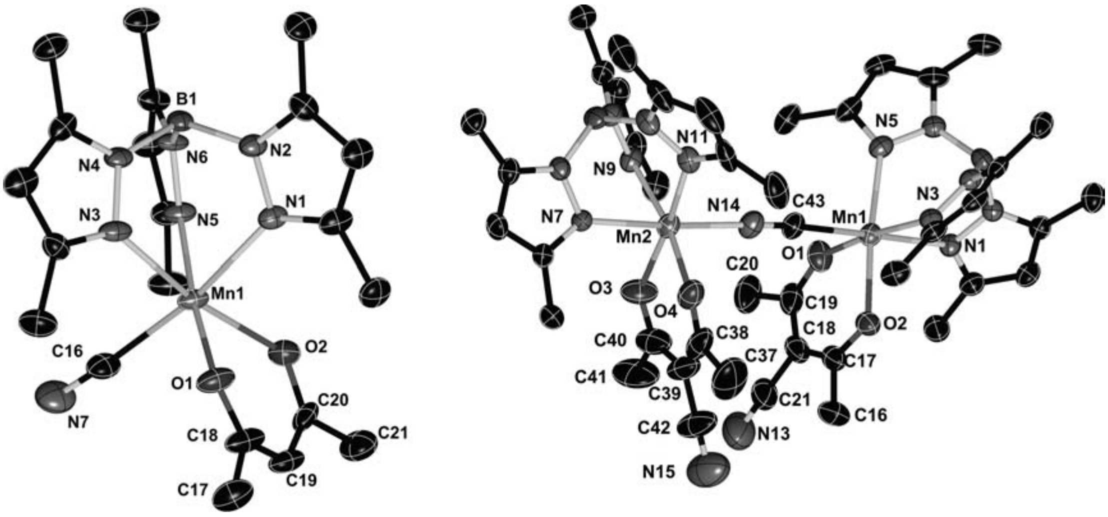

**Figure 1.** X-ray structures of anionic portions of **1** (left) and **3** (right). Thermal ellipsoids are at the 50% level, and all hydrogen atoms, cations, and lattice solvent are removed for clarity.

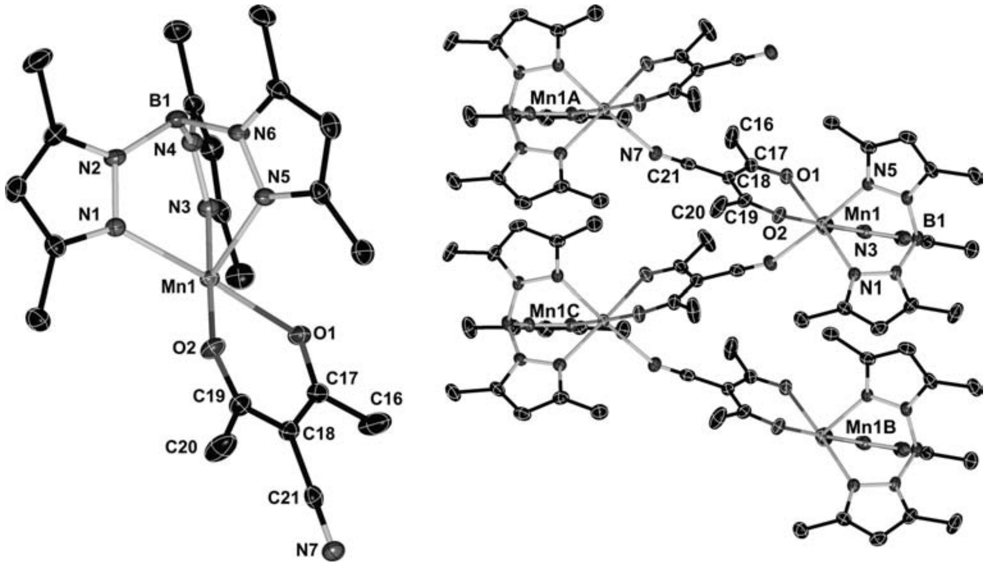

**Figure 2.** Truncated X-ray structures of (left) asymmetric unit and (right) zigzag chain in **2**. Thermal ellipsoids are at the 50% level, and all hydrogen atoms and lattice solvent are removed for clarity.

the sole cyanide-containing complex, while $[(\mathrm{Tp}^*)_2\mathrm{Mn}^{\mathrm{II}}]$ is the only isolable pyrazolylborate complex. Similarly, treatment of **7** with $\mathrm{Co}^{\mathrm{II}}(\mathrm{OTf})_2$ and two equivalents of 2,2′-bipyridine affords a mixture of reaction products regardless of reaction temperature. From these studies, we infer that facile cyanide redistribution and electron transfer prevents the formation of the desired $\{\mathrm{Mn}^{\mathrm{III}}{}_2\mathrm{Co}^{\mathrm{II}}{}_2\}$ complex.

**Crystallographic Studies: Divalent Complexes.** Yellow crystals of **1** are found in the monoclinic $P2_1/n$ space group (Table 1 and Figure 1, left). The pseudo-$C_s$-symmetric six-coordinate anions exhibit Mn−C and Mn−O bond distances of 2.248(8) [Mn1−C16], 2.162(5) [Mn1−O1], and 2.227(5) [Mn1−O2], while the Mn−N distances range from 2.263(5) to 2.286(5) Å (Table 2). In **1**, the $\kappa^2$-*O*,*O*′-acetylacetonate (acac) ligand C−O bond lengths are identical [1.261(6) Å], while the C18−C19 and C19−C20 [1.40(1) Å] distances are equivalent (Table 2). The O1−Mn1−O2, Mn1−O1−C18, and Mn1−O2−C20 bond angles are 83.3(2), 126.8(5), and 124.7(5)°, while the Mn1−C16−N7 and C16−Mn1−N1 angles are nearly linear, being 176.5(5) and 171.5(2)°, respectively (Table 3). The manganese, O1, and O2 centers are ca. −0.167(4), +0.171(4), and +0.145 Å above the mean Mn1−O1−C18−C19−C20−O2 plane, suggesting that torsional twisting (*ca.* 22°) of the acetylacetonate may result from steric interactions with the Tp* ligand methyl group (C1) directed toward the Mn(acac) plane; the closest contact is 3.382(1) Å [C1···O1].

Compound **2** crystallizes in the monoclinic $P2_1/c$ space group as a zigzag one-dimensional chain that propagates along the crystallographic *c* direction (Table 1 and Figure 2). The Mn1−O1 and Mn1−O2 distances [2.156(1) and 2.195(1) Å] are slightly shorter than those in **1**, while the Mn−N7 bond is 2.315(2) Å (Table 2). The O1−Mn1−O2 bond angle is

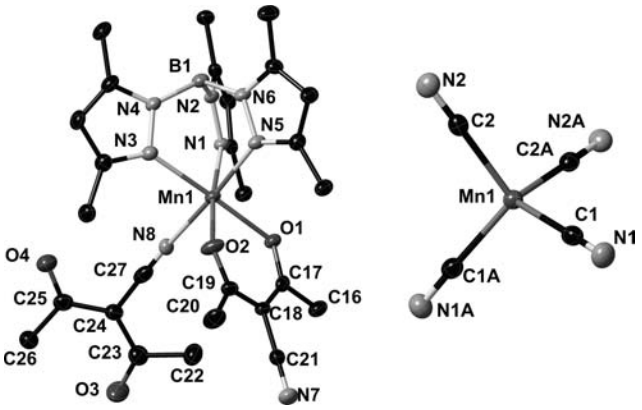

**Figure 3.** X-ray structures of the anionic portion of **4** (left) and **5** (right). Thermal ellipsoids are at the 50% level, and all hydrogen atoms, cations, and lattice solvent are removed for clarity.

80.93(5)°, while the Mn1−O1−C17 and Mn1−O2−C19 angles are comparable at 130.7(1) and 129.5(1)°, respectively; the bridging nitrile Mn1A−N7−C21 and C17−C18−C19 angles are also distorted and are 155.0(2) and 124.8(2)°, respectively (Table 3). The $\kappa^2$-*O*,*O*′-3-cyanoacetylacetonate ligand (acac$^{3\text{-CN}}$) in **2** also adopts a twisted (*ca.* 21°) orientation, relative to the mean plane defined by the manganese and 3-cyanoacetylacetonate [Mn1, O1, C17, C18, C19 and O2] (Figure 2) that is reminiscent of those in structures of **1**. The Mn$^{\text{II}}$ and oxygen atoms are −0.160(1), 0.153(1), and 0.152(1) Å from this plane, respectively, while C16 and C20 are nearly coplanar. The 3-cyanoacetylacetonate is also bent away from the Tp* methyl group projecting above and toward the Mn($\kappa^2$-acac$^{3\text{-CN}}$) plane [155.0 (1)°, Mn1−N7−C21], and the closest O···C contacts are *ca.* 3.328(1) Å.

Compound **3** crystallizes in the triclinic $P\bar{1}$ space group and consists of two neutral [(Tp*)Mn$^{\text{II}}$($\kappa^2$-acac$^{3\text{-CN}}$)] fragments linked via a single $\mu$-CN bridge (Table 1 and Figure 1, right), which resides on a crystallographic inversion center. The bridging cyanide carbon and nitrogen atom sites are disordered along the Mn1···Mn2 vector, and nearly identical Mn1−C43(N14) and Mn2−N14(C43) bond lengths [2.241(4) Å] are found (Table 2). Consistent with this assumption, the Mn−(CN) distances in **3** are longer than those seen in $\text{Na}_4[\text{Mn}^{\text{II}}(\text{CN})_6]\cdot 10\text{H}_2\text{O}$ [1.95(1) Å, Mn−C], $[\text{Mn}^{\text{II}}(\text{HL})(\text{OH}_2)][\text{Mn}^{\text{III}}(\text{CN})_6]\cdot 2\text{H}_2\text{O}$ (L = 1,2-diaminopropane) [2.197(1) to 2.232(1) Å], and the Mn−N$_{\text{MeCN}}$ bonds present in $[\text{Mn}^{\text{II}}(\text{bptz})(\text{NCMe})_2][\text{BF}_4]_2$ [2.143(4) and 2.166(4) Å; bptz = 3,6-bis(2-pyridyl)-1,2,4,5-tetrazine].[64,65,112]

The structural features of the 3-cyanoacetylacetonate fragments in **3** are nearly identical, and their bonds are comparable to a variety of substituted analogues.[97−100] The O−C bonds range from 1.250(4) [O2−C17] to 1.261(5) [O3−C40] Å, while the C17−C18−C19 and C38−C39−C40 bond angles are 125.7(4) and 125.5(4)°, respectively (Tables 2 and 3). The acac$^{3\text{-CN}}$ fragments in **3** are canted toward each other relative to the Mn1−C43−N14−Mn2 axis, and the cyano groups are rotated by *ca.* 14.5° (Figure 1, right) from an eclipsed conformation. The close acac$^{3\text{-CN}}$ ligand contacts [3.605(5) Å] are likely the result of steric pressure from adjacent Tp* methyl groups [*ca.* 3.620(5) Å].

Compound **4** crystallizes in the monoclinic $P2_1/n$ space group as a six-coordinate complex that is structurally related to **1**−**3** (Table 1 and Figure 3, left). Charge balance considerations suggest that **4** contains a Mn$^{\text{II}}$ center, two anionic 3-cyanoacetylacetonates, and a Tp*$^-$ anion (as shown below magnetic data confirm this assumption). The 3-cyanoacetylacetonate ligands adopt $\eta^1$-NC-acac and $\kappa^2$-acac$^{3\text{-CN}}$ conformations, respectively (Figure 3, right), and a distorted octahedral coordination environment is found for **4**. The O1−Mn1−O2 and C17−C18−C19 angles are rather acute [81.05(5) and 125.2(2)°], while the N1−Mn1−N8 and N1−Mn1−O1 ones are 94.21(7) and 95.05(6)°, respectively. The acac$^{3\text{-CN}}$ ligands are nearly planar, and bond angles of 125.2(2) [C17−C18−C19] and 127.2(2)° [C23−C24−C25] are found (Table 3).

The structural data also suggest that negative charge delocalization within the 3-cyanoacetylacetonates may be dependent on how they coordinate to the manganese ion in **4**. The C−O distances are slightly shorter within the $\eta^1$-3-cyanoacetylacetonate ($\eta^1$-NC-acac), and an anti- orientation of the carbonyl groups is found, with C−O bonds ranging between 1.226(2) [C23−O3] and 1.253(2) Å [C17−O1]. The C24−C25, C24−C23, and C24−C27 [1.442(2), 1.445(2), and 1.443(2) Å] distances are also slightly longer in the $\eta^1$-NC-acac fragment, relative to those in the $\kappa^2$-acac$^{3\text{-CN}}$ unit [1.429(2) Å, C17−C18 and C18−C19; 1.434(2) Å, C18−C21], while the cyano C−N distances differ only slightly for C27−N8 and C21−N7 [1.092(2) vs 1.148(3) Å], respectively (Table 2). Assuming that efficient charge delocalization within the $\kappa^2$-acac$^{3\text{-CN}}$ fragment leads to a more symmetrical bonding arrangement, the Mn1−O1 and Mn1−O2 distances are also comparable [2.159(1) and 2.178(2) Å], while the Mn1−N8$_{\text{cyano}}$ distance is slightly shorter than those in **2** [2.256(3) vs 2.315(2) Å]. As judged from the metrical parameters, we tentatively conclude that the negative ligand charge is localized onto C24 within the $\eta^1$-3-NC-acac fragment, while it is delocalized throughout the $\kappa^2$-acac$^{3\text{-CN}}$ ligand in **4** (Table 2).

Compounds **5** and **9** crystallize in the monoclinic ($C2/c$) and tetragonal ($I\bar{4}$) space groups, respectively, and represent rare examples of divalent homoleptic cyanomanganates (Table 4).[64,65,76] Crystals of **5** contain four-coordinate $[\text{Mn}^{\text{II}}(\text{CN})_4]^{2-}$ anions with Mn−C distances ranging between 2.137(2) [Mn1−C1] and 2.151(2) Å [Mn1−C2] and C−N bonds of ca. 1.152(3) Å. The C1−Mn1−C2 bond angle [111.47(7)°] deviates slightly from ideal tetrahedral symmetry (Figure 3, right) and is comparable to those seen for $[\text{PPN}]_2[\text{Mn}^{\text{II}}(\text{CN})_4]$.[76] Complex **9** crystallizes in the tetragonal $I\bar{4}$ space group (Table 4 and Figure S1, Supporting Information) and is, to our knowledge, the first crystallographically characterized hexacyanomanganate(II) devoid of alkali metal cations.[64,65] The Mn−C distances are nearly equivalent and range from 1.960(7) Å [Mn1−C2] to 1.989(8) Å [Mn1−C1], while the C−N bonds are comparable [ca. 1.16(2) Å average]. The C1−Mn1−C1C and C1−Mn1−C2 bond angles are 90.0(1) and 179.6(6)°, indicating that **9** adopts a nearly perfect octahedral geometry (Table 4).

**Crystallographic Studies: Trivalent Complexes.** Crystals of **7** and **8** are found in the trigonal ($P3_2$) and triclinic ($P\bar{1}$) space groups, respectively (Table 4). The six-coordinate tricyano anions adopt nearly ideal $C_{3v}$ symmetry and exhibit markedly different Mn−C and Mn−N bond lengths in comparison to divalent analogues (Figure S2, Supporting Information).[116] Assuming that the Mn−C$_{\text{CN}}$ distances scale as a function of the metal center oxidation state, Mn$^{\text{III}}$ centers are expected to engage in stronger electrostatic interactions with coordinated cyanides, and the shortest Mn−C distances should be seen for **7**

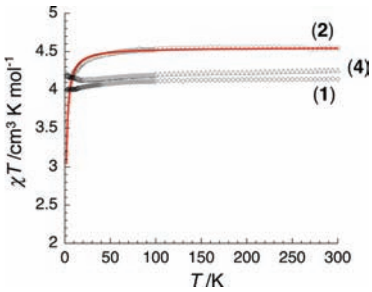

**Figure 4.** Temperature dependence of the $\chi T$ product of **1** (◇), **2** (○), and **4** (Δ) between 1.85 and 300 K at $H_{dc}$ = 1 kOe (with $\chi$ defined as the magnetic susceptibility per mole of manganese complex and equal to $M/H_{dc}$). The solid line superposed to the experimental data of **2** is the best fit using a Heisenberg chain model of classical $S$ = 5/2 spins (see text).

and **8**. Conversely, efficient $\pi$ backbonding (if present) should afford the short Mn−C$_{CN}$ distances in divalent complexes. Consistent with this assumption, the Mn−C$_{CN}$ bonds in **7** and **8** are rather short, ranging from 1.976(3) Å [for **7**] to 1.982(3) Å [for **8**], and are also considerably shorter (Table 4) than those in structures of **1** and **5**. The Mn−C distances are similar to those seen in **9** [1.986(1) Å] and [PPN]$_3$[Mn$^{III}$(CN)$_6$] [2.0020(2) Å], confirming that trivalent manganese centers are present.[75] Considering the infrared and structural data, we conclude that little $\pi$-back bonding occurs in *any* of the prepared mono- and tricyanomanganate complexes [**1**, **7**, and **8**].[103]

Given that trivalent centers are expected to have smaller ionic radii than divalent ones, tighter binding of the Mn$^{III}$ ions within the [N]$_3$ pocket of the facially coordinate Tp* ligand is anticipated. The Mn1 distance from the mean [N]$_3$ plane of the three coordinated Tp* nitrogen atoms appear to support this assumption: the Mn1−[N]$_3$ distances are 1.476(2), 1.377(2), 1.432(3) and 1.453(3), 1.403(2), 1.193(3), and 1.205(2) Å for **1**−**4**, **7**, and **8**, respectively, with the smallest values being found for **7** and **8** (Table 4).[103] Consistent with periodic trends, the average Mn−C distances in **7** and **8** [1.985(3) and 1.983(3) Å] are also shorter than those seen for early transition metal [(Tp*)M$^{III}$(CN)$_3$]$^-$ anions [e.g., Ti$^{III}$, 2.171(3) Å; V$^{IIII}$, 2.090(3) Å] and are longer than those observed when Co$^{III}$ is present [1.875(3) Å] (Table 4).[112,113] The N−Mn−N bond angles are also more acute in **7** and **8**, ranging from 89.4(1) to 90.3(1)°, while the C−Mn−C angles are between 85.8(1) and 91.7(1)°, suggesting that the Tp* ligand exerts modest steric pressure on the cyanide ligands in **7** and **8** (*vide infra*, Table 4).[103]

Complex **10** crystallizes in the monoclinic $C2/c$ space group (Table 4) and adopts a structure that is similar to {[Mn$^{II}$(CN)$_2$(bpy)$_2$]}·3H$_2$O.[102,116] For **10**, the Co−N$_{bpy}$ distances range between 1.936(5) and 1.964(5) Å and are shorter than the corresponding Mn−N bond lengths reported by Dunbar et al. [2.284(2) to 2.350(2) Å].[102] The Co1−C11 distance [1.876(6) Å] is in the range expected for complexes containing trivalent cobalt, while the C11−Co1−C11A angle [89.0(4)°] is more acute than the corresponding C−Mn−C angle [96.92(8)°] seen for [Mn$^{II}$(CN)$_2$(bipy)$_2$], being consistent with a higher positive charge and a smaller Co$^{III}$ ion (Table 4 and Figure S3, Supporting Information).[114]

**Magnetic Studies.** For **1**, **2**, and **4**, the temperature dependence of the $\chi T$ product suggests that isotropic Mn$^{II}$ ($S$ = $^5/_2$) centers are present (Figure 4). Using crushed single crystals of **1**, the $\chi T$ product remains nearly constant (~4.14 cm$^3$ K mol$^{-1}$) as the temperature is lowered from 300 to *ca.* 50 K. Below 50 K, the $\chi T$ values decrease slightly, approaching a minimum [4.01 cm$^3$ K mol$^{-1}$] at 1.8 K. Fitting the susceptibility data to the Curie−Weiss expression down to 10 K affords Curie and Weiss constants of 4.13 cm$^3$ K mol$^{-1}$ and −0.5(1) K, respectively. Lastly, fitting the field dependence of the magnetization data (collected between 1 and 7 T at 1.85 K) with an $S$ = $^5/_2$ Brillouin function confirms that **1** contains isotropic and quasi-isolated ($g$ = 1.93) Mn$^{II}$ ions (Figures S4, Supporting Information).[38,40]

Compound **2** exhibits magnetic behavior that is consistent with the presence of weakly interacting isotropic Mn$^{II}$ centers. As the temperature is lowered from 300 toward 33 K, the $\chi T$ values gradually decrease from 4.55 to 4.42 cm$^3$ K mol$^{-1}$ and then sharply approach a minimum of 3.07 cm$^3$ K mol$^{-1}$ at 1.8 K. The $\chi T$ vs $T$ data for **2** were also modeled using a modified version of a classical $S$ = 2 Heisenberg chain (eq 1):[110,114]

$$\chi = \frac{Ng^2\mu_B^2 S(S+1)}{3k_BT}\,\frac{1+u}{1-u} \qquad (1)$$

where $u = \coth(K) - 1/K$, $K = 2JS(S+1)/kT$, $S$ = $^5/_2$, and an exchange Hamiltonian of $H = -2J\,\Sigma S_iS_{i+1}$ were used. The calculated values for $J_{Mn\cdots Mn}/k_B$ and $g$ are −0.062(5) K and 2.04(2), respectively;[116] this result suggests that **2** contains isotropic and magnetically quasi-isolated Mn$^{II}$ ions.[114,115] Further support for this assumption is found in the field dependence of the magnetization at 1.85 K that rapidly approaches saturation [5.39 $\mu_B$] at 7 T, confirming that isotropic $S$ = $^5/_2$ Mn$^{II}$ centers are present (Figure S5, Supporting Information).

Likewise the $\chi T$ vs $T$ data for **4** indicate that isotropic Mn$^{II}$ ions are also present (Figures 4). At room temperature, the $\chi T$ product is 4.25 cm$^3$ K mol$^{-1}$ and slowly approaches a slightly smaller value [4.13 cm$^3$ K mol$^{-1}$ at 16 K] as the temperature decreases. At lower temperatures, the $\chi T$ values increase slightly and reach a maximum of 4.20 cm$^3$ K mol$^{-1}$ at 1.8 K. The $\chi T$ product is very weakly temperature dependent following roughly a Curie law with $C$ = 4.15 cm$^3$ K mol$^{-1}$, confirming that **4** contains isotropic quasi-isolated $S$ = $^5/_2$ Mn$^{II}$ centers. Consistent with this assumption, at 1.8 K, the saturation magnetization data collected for **4** quickly approach a maximum value of 4.71 $\mu_B$ at an applied magnetic field of 7 T (Figures S6 and S7, Supporting Information).

Consistent with previously described infrared and structural data, the magnetic measurements suggest that **7** is an authentic tricyanomanganate(III) complex.[103] The room temperature $\chi T$ value [1.1 cm$^3$ K mol$^{-1}$] of **7** is close to the value expected for a complex containing Mn$^{III}$ ions ($S$ = 1). In comparison, values reported for either [PPN]$_2$[Mn$^{II}$(CN)$_4$] or [PPN]$_3$[Mn$^{III}$(CN)$_6$] (4.49 and 1.98 cm$^3$ K mol$^{-1}$) are much higher, which suggests that trivalent ions are present and that orbital contributions to the spin ground state are nearly absent in **7**.[3,75,76,103] The temperature dependence of the $\chi T$ data follows Curie behavior down to ca. 100 K and then decreases further toward a minimum of 0.15 cm$^3$ K mol$^{-1}$ at 1.8 K. An anisotropic Heisenberg Hamiltonian ($H = DS_{Mn}{}^2$) can be used to fit the experimental data, and $g$ and $D/k_B$ parameters of 2.09(2) and +9.4(2) K are found, respectively.[103] The unexpectedly large $D$ parameter is probably due to antiferromagnetic intercomplex interactions, and this assumption is supported by the $M$ vs $H$ data collected below 8 K, in that the same $D$ value is not reproduced when using an anisotropic Heisenberg model.[103,116] Additionally, compound

**7** remains EPR silent down to 2 K and consistent with behavior expected for complexes containing an integer spin ion.

Further evidence in support of an $S = 1$ ground state for **7** can be found in extended Hückel tight-binding (EHTB) calculations.[103] The $d(xz)$ and $d(yz)$ orbitals lie close in energy to the $d(z^2)$ orbital (225 and 267 meV above, respectively), and **7** concomitantly adopts an $S_T = 1$ spin ground state. Significant $\pi$-type spin density is found to be delocalized into the Tp* and cyanide ligands, and short H···H and H···NC−Mn contacts (ca. 2.4 and 2.7 Å) are also found between adjacent $[(\mathrm{Tp}^*)\mathrm{Mn}(\mathrm{CN})_3]^-$ anions. We propose that these short intercomplex contacts may allow for antiferromagnetic interactions and explain the unusual appearance of the $\chi T$ data seen for **7** at low temperatures.

## CONCLUSIONS

Manganese pyrazolylboates are easily prepared from substituted 2,4-pentanediones under mild reaction conditions. These complexes exhibit rich reactivity under oxidative and metathesis reaction conditions and can be used to prepare new paramagnetic mono- and tricyanomanganate complexes. The divalent complexes exhibit isotropic $S = {}^5/_2$ spin ground states, while the corresponding $C_{3v}$-symmetric tricyanomanganate(III) complexes adopt a $S = 1$ spin states. These results highlight the role that symmetry and orbital degeneracy play in introducing orbital angular momentum contributions to the magnetic ground state of structurally related tricyanometalate anions.

## ASSOCIATED CONTENT

Ⓢ **Supporting Information.** Additional magnetic (Figures S4−S10) and X-ray crystallographic (Figures S1−S3; CIF format, **1**−**5**) and **7**−**10** data. This material is available free of charge via the Internet at http://pubs.acs.org.

## AUTHOR INFORMATION

### Corresponding Author

*E-mail: holmesst@umsl.edu (S.M.H.).

### Present Addresses

○Department of Chemistry Biochemistry, University of Missouri—St. Louis, St. Louis, Missouri 63121, United States

## ACKNOWLEDGMENT

S.M.H. gratefully acknowledges the National Science Foundation (CAREER, CHE-0914935) and the University of Missouri—St. Louis for financial support. Sean Parkin is also thanked for access to the University of Kentucky X-ray facility and G.T.Y. acknowledges Virginia Tech and the National Science Foundation (CHE-023488) for partial support for the purchase of a Quantum Design MPMS XL magnetometer. M.H.W. acknowledges the U.S. Department of Energy (DE-FG02-86ER45259). R.C. thanks the University of Bordeaux, the ANR (NT09_469563, AC-MAGnets), the Région Aquitaine, the GIS Advanced Materials in Aquitaine (COMET Project), and the CNRS (PICS No. 4659) for financial support. The authors are also grateful to Christopher J. Ziegler for the acquisition of EPR data.

## REFERENCES

(1) Shores, M. P.; Sokol, J. J.; Long, J. R. *J. Am. Chem. Soc.* **2002**, *124*, 2279–2292.

(2) Sokol, J. J.; Hee, A. G.; Long, J. R. *J. Am. Chem. Soc.* **2002**, *124*, 7656–7657.

(3) (a) Berlinguette, C. P.; Vaughn, D.; Cañada-Vilalta, C.; Galán-Mascarós, J.-R.; Dunbar, K. R. *Angew. Chem., Int. Ed.* **2003**, *42*, 1523–1526. (b) Palii, A. V.; Ostrovsky, S. M.; Klokishner, S. I.; Tsukerblat, B. S.; Berlinguette, C. P.; Dunbar, K. R.; Galán-Mascarós, J. R. *J. Am. Chem. Soc.* **2004**, *126*, 16860–16867.

(4) (a) Schelter, E. J.; Prosvirin, A. V.; Reiff, W. M.; Dunbar, K. R. *Angew. Chem., Int. Ed.* **2004**, *43*, 4912–4915. (b) Schelter, E. J.; Prosvirin, A. V.; Dunbar, K. R. *J. Am. Chem. Soc.* **2004**, *126*, 15004–15005.

(5) Li, D.; Parkin, S.; Wang, G.; Yee, G. T.; Prosvirin, A. V.; Holmes, S. M. *Inorg. Chem.* **2005**, *44*, 4903–4905.

(6) Li, D.; Parkin, S.; Wang, G.; Yee, G. T.; Holmes, S. M. *Inorg. Chem.* **2005**, *45*, 1951–1959.

(7) Li, D.; Parkin, S.; Wang, G.; Yee, G. T.; Holmes, S. M. *Inorg. Chem.* **2006**, *45*, 2773–2775.

(8) Li, D.; Clérac, R.; Parkin, S.; Wang, G.; Yee, G. T.; Holmes, S. M. *Inorg. Chem.* **2006**, *45*, 5251–5253.

(9) Li, D.; Parkin, S.; Wang, G.; Yee, G. T.; Clérac, R.; Wernsdorfer, W.; Holmes, S. M. *J. Am. Chem. Soc.* **2006**, *128*, 4214–4215.

(10) Park, K.; Holmes, S. M. *Phys. Rev. B* **2006**, *74*, 224440.

(11) Li, D.; Clérac, R.; Parkin, S.; Wang, G.; Yee, G. T.; Holmes, S. M. *Inorg. Chem.* **2006**, *45*, 7569–7571.

(12) Li, D.; Parkin, S.; Clérac, R.; Wang, G.; Yee, G. T.; Holmes, S. M. *Eur. J. Inorg. Chem.* **2007**, 1341–1346.

(13) Wang, S.; Zuo, J.-J.; Zhou, H.-C.; Choi, H. J.; Ke, Y.; Long, J. R.; You, X.-Z. *Angew. Chem., Int. Ed.* **2004**, *43*, 5940–5943.

(14) Wang, S.; Wang, S.; Zuo, J.-L.; Zhou, H.-C.; Song, Y.; Gao, S.; You, X.-Z. *Eur. J. Inorg. Chem.* **2004**, 3681–3687.

(15) Kim, J.; Han, S.; Cho, I.-K.; Choi, K. Y.; Heu, M.; Yoon, S.; Suh, B. J. *Polyhedron* **2004**, *23*, 1333–1339.

(16) Wang, S.; Zuo, J.-L.; Zhou, H.-C.; Song, Y.; You, X.-Z. *Inorg. Chim. Acta* **2005**, *358*, 2101–2106.

(17) Beltran, L. M. C.; Long, J. R. *Acc. Chem. Res.* **2005**, *38*, 325–334.

(18) Sessoli, R.; Gatteschi, D. *Angew. Chem., Int. Ed.* **2003**, *42*, 268–297.

(19) Leuenberger, M. N.; Loss, D. *Nature* **2001**, *410*, 789–793.

(20) Wernsdorfer, W.; Aliaga-Alcalde, N.; Hendrickson, D. N.; Christou, G. *Nature* **2002**, *416*, 406–409.

(21) Hill, S.; Edwards, R. S.; Aliaga-Alcalde, N.; Christou, G. *Science* **2003**, *302*, 1015–1018.

(22) Caneschi, A.; Gatteschi, D.; Sessoli, R.; Barra, A.-L; Brunel, L.-C; Guillot, M.; Sun, Z.; Grant, C. M.; Castro, S. L.; Hendrickson, D. N.; Christou, G. *Chem. Commun.* **1998**, 721–722.

(23) Sessoli, R.; Gatteschi, D.; Caneschi, A.; Novak, M. A. *Nature* **1993**, *365*, 141–143.

(24) Aubin, S. M. J.; Dilley, N. R.; Wemple, M. W.; Maple, M. B.; Christou, G.; Hendrickson, D. N. *J. Am. Chem. Soc.* **1998**, *120*, 839–840.

(25) Barra, A. L.; Caneschi, A.; Cornia, A.; Fabrizi de Biani, F.; Gatteschi, D.; Sangregorio, C.; Sessoli, R.; Sorace, L. *J. Am. Chem. Soc.* **1999**, *121*, 5302–5310.

(26) Caneschi, A.; Gatteschi, D.; Sessoli, R.; Barra, A. L.; Brunel, L. C.; Guillot, M. *J. Am. Chem. Soc.* **1991**, *113*, 5873–5874.

(27) Aubin, S. M. J.; Wemple, M. W.; Adams, D. M.; Tsai, H.-L.; Christou, G.; Hendrickson, D. N. *J. Am. Chem. Soc.* **1996**, *118*, 7746–7754.

(28) Ruiz, D.; Sun, Z.; Albela, B.; Folting, K.; Ribas, J.; Christou, G.; Hendrickson, D. N. *Angew. Chem., Int. Ed.* **1998**, *37*, 300–302.

(29) Murugesu, M.; Habrych, M.; Wernsdorfer, W.; Abboud, K. A.; Christou, G. *J. Am. Chem. Soc.* **2004**, *126*, 4766–4767.

(30) Lescouëzec, R.; Vaissermann, J.; Lloret, F.; Julve, F.; Verdaguer, M. *Inorg. Chem.* **2002**, *41*, 5943–5945.

(31) (a) Schelter, E. J.; Bera, J. K.; Basca, J.; Galán-Mascarós, J. R.; Dunbar, K. R. *Inorg. Chem.* **2003**, *42*, 4256–4258. (b) Dunbar, K. R.;

Schelter, E. J.; Palii, A. V.; Ostrovsky, S. M.; Mirovitskii, V. Y.; Hudson, J. M.; Omary, M. A.; Klokishner, S. I.; Tsukerblat, B. S. *J. Phys. Chem. A* **2003**, *107*, 11102–11111.

(32) Li, D.; Ruschman, C.; Parkin, S.; Clérac, R.; Holmes, S. M. *Chem. Commun.* **2006**, 4036–4038.

(33) Sato, O.; Tao, J.; Zhang, Y.-Z. *Angew. Chem., Int. Ed.* **2007**, *46*, 2152–2187.

(34) Funck, K. E.; Hilfiger, M. G.; Berlinguette, C. P.; Shatruk, M.; Wernsdorfer, W.; Dunbar, K. R. *Inorg. Chem.* **2009**, *48*, 3438–3452.

(35) (a) Li, D.; Clérac, R.; Roubeau, O.; Harté, E.; Mathonière, C.; Le Bris, R.; Holmes, S. M. *J. Am. Chem. Soc.* **2008**, *130*, 252–258. (b) Li, D.; Clérac, R.; Roubeau, O.; Harté, E.; Mathonière, C.; Le Bris, R.; Holmes, S. M. Unpublished work. (c) Zhang, Y.; Li, D.; Clérac, R.; Kalisz, M.; Mathonière, C.; Holmes, S. M. *Angew. Chem., Int. Ed.* **2010**, *49*, 3752–3756.

(36) Wang, S.; Zuo, J.-L.; Gao, S.; Zhou, H.-C.; Zhang, Y.-Z.; You, X.-Z. *J. Am. Chem. Soc.* **2004**, *126*, 8900–8901.

(37) Kahn, O. *Molecular Magnetism*; VCH Publishers: New York, 1993.

(38) Carlin, R. L. *Magnetochemistry*; Springer-Verlag: New York, 1986.

(39) Wertz, J. E.; Bolton, J. R. *Electron Spin Resonance: Elementary Theory and Practical Applications*; Chapman and Hall: New York, 1986.

(40) Boudreaux, E. A.; Mulay, L. N. *Theory and Applications of Molecular Paramagnetism*; Wiley: New York, 1976.

(41) Entley, W. R.; Girolami, G. S. *Inorg. Chem.* **1994**, *33*, 5165–5166.

(42) Behrens, H.; Linder, E.; Schindler, H. *Z. Anorg. Allg. Chem.* **1969**, *365*, 119.

(43) Manchot, W.; Gall, H. *Ber.* **1928**, *61*, 1135.

(44) Grube, G.; Brause, W. *Ber.* **1927**, *60*, 2273.

(45) Qureshi, A. M.; Sharpe, A. G. *The Chemistry of Cyano Complexes of the Transition Metals*; Academic: New York, 1976.

(46) Cotton, F. A.; Monchamp, R. R.; Henry, R. J. M.; Young, R. C. *J. Inorg. Nucl. Chem.* **1959**, *10*, 28–38.

(47) Hieber, W.; Nast, R.; Proeschel, E. *Z. Anorg. Chem.* **1948**, *256*, 159–168.

(48) Miki, E.; Kubo, S.; Mizumachi, K.; Ishimori, T.; Okuno, H. *Bull. Chem. Soc. Jpn.* **1971**, *44*, 1024–1027.

(49) Fenske, R. F.; De Kock, R. L. *Inorg. Chem.* **1972**, *11*, 437–444.

(50) Chiswell, B.; Venanzi, L. M. *J. Chem. Soc. A* **1966**, 417–419.

(51) Behrens, H.; Ranly, H. J.; Lindner, E. *Z. Anorg. Allg. Chem.* **1974**, *409*, 299–310.

(52) Hieber, W.; Schropp, W., Jr. *Z. Naturforsch.* **1959**, *14B*, 460–461.

(53) Behrens, H.; Ruyter, E.; Lindner, E. *Z. Anorg. Allg. Chem.* **1967**, *349*, 251–257.

(54) Manchot, W.; Gall, H. *Ber. Deutsch. Chem. Ges.* **1928**, *61B*, 1135–1140.

(55) Grube, G.; Brause, W. *Ber. Deutsch. Chem. Ges.* **1927**, *60B*, 2273–2278.

(56) Treadwell, W. D.; Raths, W. E. *Helv. Chim. Acta* **1952**, *35*, 2259–2275.

(57) Clauss, D.; Lissner, A. *Z. Anorg. Allg. Chem.* **1958**, *297*, 300–310.

(58) (a) Hieber, W.; Nast, R.; Floss, J. G. *Z. Anorg. Allg. Chem.* **1956**, *283*, 188–195. (b) Hauck, J. *Inorg. Nucl. Chem. Lett.* **1976**, *12*, 893–896.

(59) Griffith, W. P.; Turner, G. T. *J. Chem. Soc. A* **1970**, *6*, 858–862.

(60) Krasser, W.; Bohres, E. W.; Schwochau, K. *Z. Naturforsch.* **1972**, *27*, 1193–1196.

(61) Caglioti, V.; Sartori, G.; Scrocco, M. *Atti Accad. Nazl. Lincei, Rend., Classe Sci. Fis., Mat. Nat.* **1957**, *22*, 266–268.

(62) Kolodziej, H. A.; Sorriso, S. *Chem. Phys.* **1983**, *77*, 341–347.

(63) (a) Tullberg, A.; Vannerberg, N. G. *Acta Chem. Scand.* **1967**, *21*, 1462–1472. (b) Ziegler, B.; Witzel, M.; Babel, D. *Z. Anorg. Alleg. Chem.* **1991**, *600*, 239–248.

(64) Tullberg, A.; Vannerberg, N. G. *Acta Chem. Scand.* **1971**, *25*, 343–344.

(65) Tullberg, A.; Vannerberg, N. G. *Acta Chem. Scand.* **1974**, *28*, 551–562.

(66) Qureshi, A. M.; Sharpe, A. G. *J. Inorg. Nucl. Chem.* **1968**, *30*, 2269–2270.

(67) Figgis, B. N. *Trans. Faraday Soc.* **1961**, *57*, 198–204.

(68) Vannerberg, N. G. *Acta Chem. Scand.* **1970**, *24*, 2335–2348.

(69) Gupta, M. P.; Milledge, H. J.; McCarthy, A. E. *Acta Crystallogr., Sect. B* **1974**, 656–661.

(70) Cooke, A. H.; Duffus, H. J. *Proc. Phys. Soc.* **1955**, *68A*, 32–34.

(71) Kamimura, H. *J. Phys. Soc. Jpn.* **1956**, *11*, 1171–1181.

(72) Udachin, Yu. M.; Dyatkina, M. E. *Zhur. Struk. Khim.* **1967**, *8*, 145–153.

(73) Chawla, I. D.; Frank, M. J. *J. Inorg. Nucl. Chem.* **1970**, *32*, 555–563.

(74) Lower, J. A.; Conrad, F. W. *Inorg. Synth.* **1946**, *2*, 213–214.

(75) Buschmann, W. E.; Liable-Sands, L.; Rheingold, A. L.; Miller, J. S. *Inorg. Chim. Acta* **1999**, *284*, 175–179.

(76) Buschmann, W. E.; Arif, A. M.; Miller, J. S. *Angew. Chem., Int. Ed.* **1998**, *37*, 781–783.

(77) Manson, J. L.; Buschmann, W. E.; Miller, J. S. *Inorg. Chem.* **2001**, *40*, 1926–1935.

(78) Silvernail, C. M.; Yap, G.; Sommer, R. D.; Rheingold, A. L.; Day, V. W.; Belot, J. A. *Polyhedron* **2001**, *20*, 3113–3117.

(79) Rasmussen, J. K.; Hassner, A. *Synthesis* **1973**, *11*, 682.

(80) Magnus, P. D.; Payne, A. H. U.S. Patent Application Publ. 2002, US 20021220170 A120020829; CAN 137:185103 AN 2002:658795

(81) Mehrota, R. C. *Metal β-Diketonates and Allied Derivatives*, Academic: New York, 1978 and references cited therein.

(82) Harris, C. M.; McKenzie, E. D. *J. Inorg. Nucl. Chem.* **1961**, *19*, 372–375.

(83) Davis, T. S.; Fackler, J. P.; Weeks, M. J. *Inorg. Chem.* **1968**, *7*, 1994–2002.

(84) Bhattacharjee, M. N.; Chaudhuri, M. K.; Khathing, D. T. *J. Chem. Soc., Dalton Trans.* **1982**, 669–670.

(85) Gritzner, G.; Muraner, H.; Gutmann, V. *J. Electroanal. Chem.* **1979**, *101*, 185–200.

(86) Yamaguchi, K.; Sawyer, D. T. *Inorg. Chem.* **1985**, *24*, 971–976.

(87) Richert, S. A.; Tsang, P. K. S.; Sawyer, D. T. *Inorg. Chem.* **1988**, *27*, 1814–1818.

(88) Richert, S. A.; Tsang, P. K. S.; Sawyer, D. T. *Inorg. Chem.* **1989**, *28*, 2471–2475.

(89) Saha, A.; Musie, G.; Powell, D. R. *Acta Crystallogr.* **2005**, *E61*, m1144–m1146.

(90) Morosin, B.; Brathovde, J. R. *Acta Crystallogr.* **1964**, *17*, 705–711.

(91) Stults, B. R.; Marianelli, R. S.; Day, V. W. *Inorg. Chem.* **1979**, *18*, 1853–1881.

(92) Geremic, S.; Demitri, N. *J. Chem. Educ.* **2005**, *82*, 460–465.

(93) Lawson, K. E. *Spectrochim. Acta* **1961**, *17*, 248–258.

(94) Fackler, J. P.; Davis, T. S.; Chawla, I. D. *Inorg. Chem.* **1965**, *4*, 130–132.

(95) Fleming, C. A.; Thornton, D. A. *J. Mol. Sci.* **1973**, *17*, 79–89.

(96) Thornton, D. A. *J. Mol. Struct.* **1971**, *10*, 39–48.

(97) Trofimenko, S.; Long, J. R.; Nappier, T.; Shore, S. G. *Inorg. Synth.* **1970**, *12*, 99–107.

(98) Trofimenko, S. *Scorpionates, The Coordination Chemistry of Polypyrazolylborate Ligands*; Imperial College Press: London, 1999 and references therein.

(99) Mashima, K.; Oshiki, T.; Tani, K. *Organometallics* **1997**, *16*, 2760–2762.

(100) Andreades, S.; Zahnow, E. W. *J. Am. Chem. Soc.* **1969**, *91*, 4181–4190.

(101) Holmes, S. M. Ph.D. Thesis, University of Illinois at Urbana-Champaign, Urbana, IL, 1999.

(102) Smith, J. A.; Galán-Mascarós, J.-R.; Clérac, R.; Sun, J.-S.; Ouyang, X.; Dunbar, K. R. *Polyhedron* **2001**, *20*, 1727–1734.

(103) Tang, M.; Li, D.; Mallik, U. P.; Withers, J. R.; Brauer, S.; Rhodes, M. R.; Clérac, R.; Yee, G. T.; Whangbo, M.-H.; Holmes, S. M. *Inorg. Chem.* **2010**, *49*, 4753–4755.

(104) Otwinowski, Z.; Minor, W. *Methods Enzymol.* **1997**, *276*, 307–326.

(105) Sheldrick, G. M. *SHELX-97*; University of Gottingen: Gottingen, Germany, 1997.

(106) Sheldrick, G. M. *SADABS*; Bruker Analytical X-ray Systems: Madison, WI, 1996.

(107) *International Tables for Crystallography*; Kluwer Academic Publishers: Dordrecht, The Netherlands, 1992; Vol. C.

(108) Nakamoto, K. *Infrared and Raman Spectra of Inorganic and Coordination Compounds*, 5th ed, Part B; Wiley: New York, 1997; pp 54−58; 105−116.

(109) Entley, W. R. Ph.D. Thesis, University of Illinois at Urbana-Champaign, Urbana, IL, 1990.

(110) Chanaka, D.; De Alwis, D. C. L; Schultz, F. A. *Inorg. Chem.* **2003**, *42*, 3616–3622.

(111) Ohba, M.; Fukita, N.; Ōkawa, H. *J. Chem. Soc., Dalton Trans.* **1997**, 1733–1737.

(112) Colacio, E.; Ghazi, M.; Stoeckli-Evans, H.; Lloret, F.; Moreno, J. M.; Pérez, C. *Inorg. Chem.* **2001**, *40*, 4876–4883.

(113) (a) Kaneko, W.; Kitagawa, S.; Ohba, M. *J. Am. Chem. Soc.* **2007**, *129*, 248–249. (b) Campos-Fernandez, C. S.; Schottel, B. L.; Chifotides, H. T.; Bera, J. K.; Bacsa, J.; Koomen, J. M.; Russell, D. H.; Dunbar, K. R. *J. Am. Chem. Soc.* **2005**, *127*, 12909–12923.

(114) Li, D.; Withers, J. R.; Holmes, S. M. Unpublished work.

(115) Borrás-Almenar, J. J.; Burriel, R.; Coronado, E.; Gatteschi, D.; Gómez-Garcia, C. J.; Zanchini, C. *Inorg. Chem.* **1991**, *30*, 947–950.

(116) See the Supporting Information.